PHILOSOPHICAL TRANSACTIONS OF THE ROYAL SOCIETY A MATHEMATICAL, PHYSICAL & ENGINEERING SCIENCES

The Distribution of Normal Pressures on a Prolate Spheroid

R. Jones

Phil. Trans. R. Soc. Lond. A 1927 **226**, 231-266
doi: 10.1098/rsta.1927.0006

VI. *The Distribution of Normal Pressures on a Prolate Spheroid.*

By R. Jones, *M.A., D.Sc., of the Aerodynamics Department, National Physical Laboratory.*

(*Communicated by* H. Lamb, *F.R.S.*)

(Received September 22, 1926—Read November 4, 1926.)

Introductory.

During the course of certain experiments* conducted at the National Physical Laboratory in 1919, a number of observations were made of the normal pressure at points on the surface of a prolate spheroid of length/diameter ratio 4. The results were compared with the corresponding pressures, calculated by purely theoretical methods, on a similar body in rectilinear motion in an ideal fluid. The comparison showed that agreement between theory and experiment was remarkably good for three-quarters the length of the model, even when the axis of the model was inclined to the direction of motion.

The closeness of the agreement suggested that a more extensive investigation would be likely to lead to very interesting results. It was therefore decided to conduct a comprehensive series of experiments with a view to obtaining a more complete comparison. The scope of the investigation was widened to cover not only rectilinear motion which is reproduced in wind-tunnel experiments, but to include purely rotational motion (spin about a minor axis) and also motion in a circle. The whirling arm at the Laboratory provided the necessary means for reproducing this motion in the experimental part of the work.

The present paper describes the experiments which were conducted with this end in view, together with the corresponding theoretical analysis.† The matters under discussion will be considered in the following order :—

I. Theoretical Determination of the Pressures on the Spheroid.

II. Methods and Range of the Experimental Work :—

(*a*) Measurements of the pressures in rectilinear motion in a 4-foot wind tunnel.

(*b*) Measurements of the pressures with the spheroid spinning about a minor axis.

(*c*) Measurements of the pressures on the spheroid turning about an axis parallel to a minor axis, on the whirling arm.

* 'Aeronautical Research Committee, Reports and Memoranda No. 600.' "The Distribution of Pressure over the Airship Model, U721, together with a comparison with the Pressures on a Spheroid," by R. Jones and D. H. Williams.

† The work was carried out for the Aeronautical Research Committee, to whom the author is indebted for their kind permission to publish the results.

 [Published March 7, 1927.

III. Comparison of the Results—Theory and Experiment :—

(*a*) Rectilinear motion.
(*b*) Spinning motion.
(*c*) Curvilinear motion, including a comparison between rectilinear and curvilinear motion.

I. Theoretical Determination of the Pressures on the Spheroid.

1. *System of Axes and Notation* (fig. 1).

The origin O is at the centre of the spheroid.

The axis of x coincides with the major axis, positive direction forward.

The axis of y is horizontal, positive direction to starboard.

The axis of z is vertical, positive direction downwards.

Ω is the angular velocity of the spheroid about Oz.

β is the angle between the direction of the relative wind and Ox, *i.e.*, the angle of yaw of the spheroid.

V is the resultant velocity of O.

u and v are the component velocities of O along Ox and Oy.

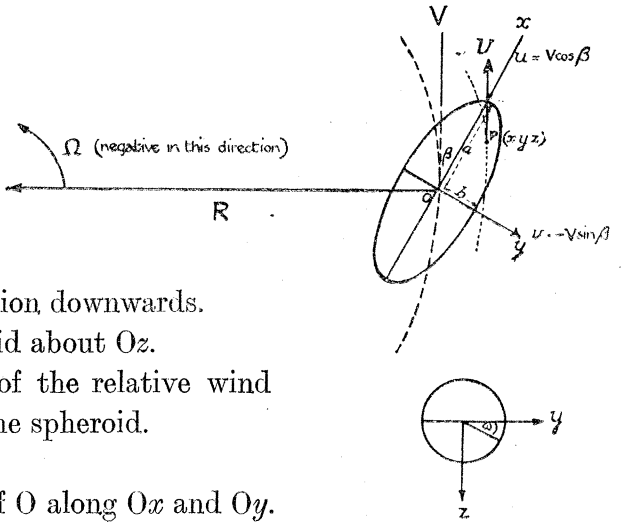

Fig. 1.—System of Axes and Notation.

$$u = \mathrm{V}\cos\beta, \qquad v = -\mathrm{V}\sin\beta.$$

a is the semi-major axis of the spheroid and b the semi-minor axis (*i.e.*, the radius of the cross-section through the centre perpendicular to a),

$$\text{the eccentricity } e = \sqrt{1 - b^2/a^2}.$$

The co-ordinates of the point P may be written, in the notation of spheroidal co-ordinates, as follows :—

$$x = ae\mu\zeta,$$
$$y = ae\sqrt{1-\mu^2}\sqrt{\zeta^2-1}\,.\cos\omega,$$
$$z = ae\sqrt{1-\mu^2}\sqrt{\zeta^2-1}\,.\sin\omega,$$

where μ, ζ and ω = constant are quadric surfaces confocal with the spheroid under consideration ($\zeta = 1/e$).

$\mu = \cos\psi$, ψ being the eccentric angle of any point P, and ω is the angular distance of P from the plane xOy.

2. The velocity potential may be written as

$$\phi = \phi_1 + \phi_2 + \phi_3 * \quad \ldots \quad (1)$$

$$\phi_1 = \frac{au}{\frac{1}{1-e^2} - \frac{1}{2e}\log\frac{1+e}{1-e}}\,\mu\left\{\tfrac{1}{2}\zeta\log\frac{\zeta+1}{\zeta-1} - 1\right\}, \quad \ldots \quad (1a)$$

$$\phi_2 = \frac{-aev}{\frac{1}{2}\log\frac{1+e}{1-e} - \frac{e-2e^3}{1-e^2}}\sqrt{1-\mu^2}\,\sqrt{\zeta^2-1}\left\{\tfrac{1}{2}\log\frac{\zeta+1}{\zeta-1} - \frac{\zeta}{\zeta^2-1}\right\}\cos\omega, \quad \ldots \quad (1b)$$

$$\phi_3 = \mathrm{A}\mu\sqrt{1-\mu^2}\,\sqrt{\zeta^2-1}\left\{\tfrac{3}{2}\zeta\log\frac{\zeta+1}{\zeta-1} - 3 - \frac{1}{\zeta^2-1}\right\}\cos\omega, \quad \ldots \quad (1c)$$

where

$$\mathrm{A} = \frac{(b^2-a^2)\,\Omega}{\frac{3}{2}\left(\frac{2}{e^2}-1\right)\log\frac{1+e}{1-e} - \frac{6}{e} + \frac{e}{1-e^2}}. \quad \ldots \quad (1d)$$

3. The pressure p at any point is given by

$$\frac{p}{\rho} = \frac{\partial\phi}{\partial t} - \tfrac{1}{2}q^2 \quad \ldots \quad (2)$$

$$q^2 = \left(\frac{\partial\phi}{\partial\mu}\cdot\frac{\partial\mu}{\partial s_\mu}\right)^2 + \text{two similar terms}, \quad \ldots \quad (3)$$

where ds_μ is a line element on the intersection of the surfaces $\zeta = \text{const.}$ and $\omega = \text{const.}$, and ϕ has the value given in (1) ... (1d).

Also

$$\frac{\partial\mu}{\partial s_\mu} = \frac{1}{ae}\sqrt{\frac{1-\mu^2}{\zeta^2-\mu^2}}, \quad \frac{\partial\zeta}{\partial s_\zeta} = \frac{1}{ae}\sqrt{\frac{\zeta^2-1}{\zeta^2-\mu^2}}, \quad \frac{\partial\omega}{\partial s_\omega} = \frac{1}{ae}\frac{1}{\sqrt{(1-\mu^2)(\zeta^2-1)}}.\dagger \quad (4)$$

4. In the equation (2) $\partial\phi/\partial t$ expresses the rate at which ϕ is increasing at a fixed point in space, whereas the value of ϕ given in (1) ... (1d) is referred to an origin which is in motion.‡

Hence in the equation (2) we put

$$\frac{\partial\phi}{\partial t} = -\left(\frac{\partial\phi}{\partial\mu}\cdot\frac{\partial\mu}{\partial s_\mu}\cdot\frac{ds_\mu}{dt}\right) - (\text{two similar terms}), \quad \ldots \quad (5)$$

ϕ on the right-hand side having the value given in (1) ... (1d).

To determine ds_μ/dt, etc., we note that the velocity components along Ox and Oy at any point (x, y, z) are $u - y\Omega$ and $v + x\Omega$ respectively.

* The values of ϕ_1, ϕ_2 and ϕ_3 are taken from 'Hydrodynamics'—Lamb, 3rd Ed., §§ 103–106.

† See 'Hydrodynamics,' *loc. cit.*

‡ 'Hydrodynamics,' § 68 following equation (7).

If the direction cosines of Ox and Oy with regard to the axes μ, ζ, ω are l_1, m_1, n_1 and l_2, m_2, n_2 respectively

$$\frac{ds_\mu}{dt} = l_1(u - y\Omega) + l_2(v + x\Omega), \qquad \frac{ds_\zeta}{dt} = m_1(u - y\Omega) + m_2(v + x\Omega), \text{ etc.}$$

5. To find l_1, m_1, n_1, l_2, m_2, n_2 we note that the equations of the surfaces $\mu = \text{const.}$ and $\omega = \text{const.}$ through a point (eccentric angle ψ) on the spheroid $\zeta = 1/e$ are

$$\mu = \text{const.} = \cos\psi\,; \qquad \frac{x^2}{(a^2 - b^2)\cos^2\psi} - \frac{y^2 + z^2}{(a^2 - b^2)\sin^2\psi} = 1,$$

$$\omega = \text{const.} = \omega\,; \qquad z = y\tan\omega.$$

The equation of the spheroid is

$$\zeta = \text{const.} = \frac{1}{e}\,, \qquad \frac{x^2}{a^2} + \frac{y^2 + z^2}{b^2} = 1.$$

On determining the direction cosines of the normals to these surfaces at the point $(a\cos\psi, b\sin\psi\cos\omega, b\sin\psi\sin\omega)$, we obtain

$$l_1 = a\sin\psi/\sqrt{a^2\sin^2\psi + b^2\cos^2\psi}, \quad m_1 = b\cos\psi/\sqrt{a^2\sin^2\psi + b^2\cos^2\psi}, \quad n_1 = 0,$$

and

$$l_2 = -b\cos\psi\cos\omega/\sqrt{a^2\sin^2\psi + b^2\cos^2\psi}, \quad m_2 = a\sin\psi\cos\omega/\sqrt{a^2\sin^2\psi + b^2\cos^2\psi},$$

$$n_2 = -\sin\omega$$

respectively.

Hence on the surface,

$$\left.\begin{aligned} \frac{ds_\mu}{dt} &= \frac{au\sin\psi - bv\cos\psi\cos\omega - ab\Omega\cos\omega}{\sqrt{a^2\sin^2\psi + b^2\cos^2\psi}} \\ \frac{ds_\zeta}{dt} &= \frac{bu\cos\psi + av\sin\psi\cos\omega + (a^2 - b^2)\,\Omega\sin\psi\cos\psi\cos\omega}{\sqrt{a^2\sin^2\psi + b^2\cos^2\psi}} \\ \frac{ds_\omega}{dt} &= -\sin\omega\,(v + a\Omega\cos\psi) \end{aligned}\right\} \quad . \quad . \quad . \quad (6)$$

6. Now let

$$\left.\begin{aligned} \frac{\frac{1}{2e}\log\frac{1+e}{1-e} - 1}{\frac{1}{2e}\log\frac{1+e}{1-e} - \frac{1}{1-e^2}} &= -\mathrm{L}, \qquad \frac{\frac{1}{2}\log\frac{1+e}{1-e} - \frac{e}{1-e^2}}{\frac{1}{2}\log\frac{1+e}{1-e} - \frac{e-2e^3}{1-e^2}} = -\mathrm{M} \\ \text{and} \qquad \frac{\frac{3}{2e}\log\frac{1+e}{1-e} - 3 - \frac{e^2}{1-e^2}}{\frac{3}{2}\frac{2-e^2}{e}\log\frac{1+e}{1-e} - 6 + \frac{e^2}{1-e^2}} &= -\mathrm{N} \end{aligned}\right\}, \quad . \quad (7)$$

then we may write

$$\left.\begin{aligned}
\frac{\partial\phi}{\partial\mu}\cdot\frac{\partial\mu}{\partial s_\mu} &= \frac{1}{\sqrt{a^2\sin^2\psi+b^2\cos^2\psi}}\Big[au\mathrm{L}\sin\psi - bv\mathrm{M}\cos\psi\cos\omega \\
&\qquad - \frac{b}{a}(a^2-b^2)\,\Omega\mathrm{N}\cos 2\psi\cos\omega\Big] \\
\frac{\partial\phi}{\partial\zeta}\cdot\frac{\partial\zeta}{\partial s_\zeta} &= \frac{1}{\sqrt{a^2\sin^2\psi+b^2\cos^2\psi}}[bu\cos\psi + av\sin\psi\cos\omega \\
&\qquad + (a^2-b^2)\,\Omega\sin\psi\cos\psi\cos\omega] \\
\text{and}\quad \frac{\partial\phi}{\partial\omega}\cdot\frac{\partial\omega}{\partial s_\omega} &= -\sin^2\omega\left[v\mathrm{M}+\frac{a^2-b^2}{a}\,\Omega\mathrm{N}\cos\psi\right]
\end{aligned}\right\}\quad . . \quad (8)$$

Whence we have (after reduction and substituting for u and v) the following expressions :—

$$p = a_0 + a_1\cos\omega + a_2\cos^2\omega + a_3\sin^2\omega + (b_1\cos\omega + b_2\cos^2\omega + b_3\sin^2\omega)\,\Omega + (c_2\cos^2\omega + c_3\sin^2\omega)\,\Omega^2, \quad . \quad . \quad . \quad (9)$$

where

$$a_0 = \tfrac{1}{2}\rho\mathrm{V}^2\cos^2\beta\left\{1 - \frac{(1+\mathrm{L})^2\sin^2\psi}{\sin^2\psi + (b^2/a^2)\cos^2\psi}\right\},$$

$$a_1 = -\tfrac{1}{2}\rho\mathrm{V}^2\frac{2\dfrac{b}{a}(1+\mathrm{L})(1+\mathrm{M})\sin\beta\cos\beta\sin\psi\cos\psi}{\sin^2\psi + (b^2/a^2)\cos^2\psi},$$

$$a_2 = \tfrac{1}{2}\rho\mathrm{V}^2\sin^2\beta\left\{1 - \frac{(b^2/a^2)(1+\mathrm{M})^2\cos^2\psi}{\sin^2\psi + (b^2/a^2)\cos^2\psi}\right\},$$

$$a_3 = \tfrac{1}{2}\rho\mathrm{V}^2\sin^2\beta\,\{1-(1+\mathrm{M})^2\},$$

$$\tfrac{1}{2}b_1\Omega = \frac{\rho\mathrm{V}^2 b}{2\mathrm{R}}\cos\beta\sin\psi\left\{\frac{(1+\mathrm{L})(1+e^2\mathrm{N}\cos 2\psi)}{\sin^2\psi + (b^2/a^2)\cos^2\psi} - 1\right\},$$

$$\tfrac{1}{2}b_2\Omega = \frac{\rho\mathrm{V}^2}{2\mathrm{R}}a\sin\beta\cos\psi\left\{\frac{(b^2/a^2)(1+\mathrm{M})(1+e^2\mathrm{N}\cos 2\psi)}{\sin^2\psi + (b^2/a^2)\cos^2\psi} - 1\right\},$$

$$\tfrac{1}{2}b_3\Omega = \frac{\rho\mathrm{V}^2}{2\mathrm{R}}a\sin\beta\cos\psi\,\{(1+\mathrm{M})(1+e^2\mathrm{N}) - 1\},$$

$$c_2\Omega^2 = \frac{a^2\rho\mathrm{V}^2}{2\mathrm{R}^2}\left\{\cos^2\psi + \frac{b^2}{a^2}\sin^2\psi - \frac{(b^2/a^2)(1+e^2\mathrm{N}\cos 2\psi)^2}{\sin^2\psi + (b^2/a^2)\cos^2\psi}\right\},$$

$$c_3\Omega^2 = \frac{a^2\rho\mathrm{V}^2}{2\mathrm{R}^2}\cos^2\psi\,\{1-(1+e^2\mathrm{N})^2\},$$

where R is the radius of the circle in which O moves, *i.e.*, $\mathrm{V} = \mathrm{R}\Omega$.

7. On substituting u for $\mathrm{V}\cos\beta$, v for $-\mathrm{V}\sin\beta$, and Ω for V/R, the terms independent of $(1+\mathrm{L})$, $(1+\mathrm{M})$, $(1+e^2\mathrm{N}\cos^2\psi)$ and $(1+e^2\mathrm{N})$, reduce to

$$\tfrac{1}{2}\rho\,(u - y\Omega)^2 + \tfrac{1}{2}\rho\,(v + x\Omega)^2,$$

or $\tfrac{1}{2}\rho \times$ (resultant velocity)^2 at the point whose co-ordinates are x and y.

Hence, putting U for the resultant velocity, we may write

$$\frac{p}{\rho} = \tfrac{1}{2}U^2 - \tfrac{1}{2}V^2\left\{\frac{(1+L)\sin\psi\cos\beta + (b/a)(1+M)\cos\psi\sin\beta\cos\omega}{\sqrt{\sin^2\psi + (b^2/a^2)\cos^2\psi}}\right\}^2$$

$$+\frac{V^2}{R}\cdot\frac{b(1+e^2N\cos 2\psi)}{\sin^2\psi+(b^2/a^2)\cos^2\psi}\{(1+L)\sin\psi\cos\beta+(b/a)(1+M)\cos\psi\sin\beta\cos\omega\}\cos\omega$$

$$-\tfrac{1}{2}\frac{V^2}{R^2}\cdot\frac{b^2(1+e^2N\cos 2\psi)^2}{\sin^2\psi+(b^2/a^2)\cos^2\psi}\cos^2\omega$$

$$-\tfrac{1}{2}V^2\sin^2\beta\sin^2\omega(1+M)^2+\frac{V^2}{R}a\sin\beta\cos\psi\sin^2\omega(1+M)(1+e^2N)$$

$$-\tfrac{1}{2}\frac{V^2}{R^2}a^2\cos^2\psi\sin^2\omega(1+e^2N)^2$$

$$=\tfrac{1}{2}U^2-\frac{V^2}{2}\left\{\frac{a(1+L)\sin\psi\cos\beta+b(1+M)\cos\psi\sin\beta\cos\omega-(ba/R)(1+e^2N\cos 2\psi)\cos\omega}{\sqrt{a^2\sin^2\psi+b^2\cos^2\psi}}\right\}^2$$

$$-\frac{V^2}{2}\sin^2\omega\{(1+M)\sin\beta-(a/R)\cos\psi(1+e^2N)\}^2 \quad (10)$$

$$=\tfrac{1}{2}U^2-\tfrac{1}{2}\left\{\left(\frac{\partial\phi}{\partial s_\mu}\right)^2+\left(\frac{\partial\phi}{\partial s_\omega}\right)^2\right\},$$

with $1+L$, $1+M$, $1+e^2N\cos 2\psi$ and $1+e^2N$ substituted for L, M, $e^2N\cos 2\psi$ and e^2N respectively.

8. When $\Omega = 0$ this expression could have been derived more simply by supposing the body reduced to rest by imposing the velocities u and v on the entire system. We should then have to add the terms ux and vy respectively to the expressions for ϕ_1 and ϕ_2 in 1a and 1b. That is, we add terms $uae\mu\zeta$ and $vae\sqrt{1-\mu^2}\sqrt{\zeta^2-1}\cos\omega$. In that case

$$p/\tfrac{1}{2}\rho V^2 = 1 - q^2, \text{ where } q^2 = \left(\frac{\partial\phi'}{\partial s_\mu}\right)^2+\left(\frac{\partial\phi'}{\partial s_\omega}\right)^2,$$

ϕ' being the new value of ϕ. $\dfrac{\partial\phi'}{\partial s_\zeta} = 0$. We then have

$$1-\frac{p}{\tfrac{1}{2}\rho V^2} = \frac{1}{V^2}\frac{1}{(a^2\sin^2\psi+b^2\cos^2\psi)}[au(1+L)\sin\psi - bv(1+M)\cos\psi\cos\omega]^2$$

$$+v^2(1+M)^2\sin^2\omega. \quad (11)$$

It is obvious that $q = 0$ when $\omega = 0$ and $\tan\psi = \dfrac{bv(1+M)}{au(1+L)}$. Let P_0 be the point at which this occurs, and let η be the inclination of the normal at this point to Ox, and ψ_0 be the value of ψ at this point.

Then

$$\tan\eta = \frac{a}{b}\tan\psi_0 = \frac{v}{u}\cdot\frac{1+M}{1+L}.$$

The maximum value of q^2 on the spheroid is

$$u^2(1+\mathrm{L})^2 + v^2(1+\mathrm{M})^2 = \mathrm{Q}^2.$$

If θ be the inclination of the normal at the point P, whose eccentric angle is ψ, to the axis Ox, $\tan\theta = (a/b)\tan\psi$.

The expression for $1 - p/\frac{1}{2}\rho\mathrm{V}^2$ may now be written in the form

$$1 - \frac{p}{\frac{1}{2}\rho\mathrm{V}^2} = \frac{u^2(1+\mathrm{L})^2 + v^2(1+\mathrm{M})^2}{\mathrm{V}^2} - \frac{\{bu(1+\mathrm{L})\cos\psi + av(1+\mathrm{M})\sin\psi\cos\omega\}^2}{\mathrm{V}^2(a^2\sin^2\psi + b^2\cos^2\psi)}$$

$$= \frac{\mathrm{Q}^2}{\mathrm{V}} - \frac{\mathrm{Q}^2}{\mathrm{V}^2}\{\cos\theta\,.\cos\eta + \sin\theta\,.\sin\eta\cos\omega\}^2. \quad \ldots\ldots\ldots\ldots \quad (12)$$

This equation is more convenient than the expressions given in (9) of § 6 for determining p in the case where $\Omega = 0$. It has accordingly been utilised for this purpose: the Ω and Ω^2 terms are best calculated from § 6.

9. *Average Pressure and Longitudinal Force.*—The average pressure at any section $x = x_0$ of the spheroid through the point P is obviously

$$\mathrm{P}' = \frac{1}{2\pi}\int_0^{2\pi} p\,.\,d\omega.$$

The part independent of Ω may be written down directly from (12)

$$\frac{\mathrm{P}'_1}{\frac{1}{2}\rho\mathrm{V}^2} = 1 - \frac{\mathrm{Q}^2}{\mathrm{V}^2} + \frac{\mathrm{Q}^2}{\mathrm{V}^2}(\cos^2\theta\cos^2\eta + \tfrac{1}{2}\sin^2\theta\sin^2\eta). \quad \ldots\ldots \quad (13)$$

The part containing V^2/R is

$$\frac{\mathrm{P}'_2}{\frac{1}{2}\rho\mathrm{V}^2} = \frac{a}{\mathrm{R}}\sin\beta\cos\psi\left[\frac{b^2(1+\mathrm{M})(1+e^2\mathrm{N}\cos 2\psi)}{a^2\sin^2\psi + b^2\cos^2\psi} - 2 + (1+\mathrm{M})(1+e^2\mathrm{N})\right], \quad (14)$$

and finally the part containing $\mathrm{V}^2/\mathrm{R}^2$

$$\frac{\mathrm{P}'_3}{\frac{1}{2}\rho\mathrm{V}^2} = \frac{1}{2}\frac{a^2}{\mathrm{R}^2}\left[\cos^2\psi + \frac{b^2}{a^2}\sin^2\psi + \cos^2\psi - \frac{b^2(1+e^2\mathrm{N}\cos 2\psi)^2}{a^2\sin^2\psi + b^2\cos^2\psi} - (1+e^2\mathrm{N})^2\right], \quad (15)$$

$$\mathrm{P}' = \mathrm{P}'_1 + \mathrm{P}'_2 + \mathrm{P}'_3.$$

The longitudinal force, *i.e.*, the force along the major axis, is

$$\int_{s_1}^{s_2}\int_0^{2\pi} p\,.\,d\omega\,.\,r\cos\theta\,.\,ds, \quad \ldots\ldots\ldots\ldots \quad (16)$$

where ds is an element of length along a section through the major axis ($s = 0$ in the plane xOy) and s_1, s_2, respectively, are values of s at the forward and after-end of the spheroid. r is the radius of the section through P perpendicular to the major axis and

$$\cos\theta = dr/ds.$$

Then the longitudinal force

$$X = \int_{0_1}^{0_2}\int_0^{2\pi} p \,.\, d\omega \,.\, r dr = \tfrac{1}{2}\int_{0_1}^{0_2}\int_0^{2\pi} p \,.\, d\omega \,.\, dr^2, \quad . \quad . \quad . \quad . \quad . \quad (17)$$

0_1 and 0_2 denoting the zero values of r at the extremities of the major axis.

10. For calculating the longitudinal force due to normal pressure, from the results of the experiments, this integral can be conveniently written in the form

$$\frac{1}{2\pi}\int_{0_1}^{0_2}\int_0^{2\pi} p \,.\, d\omega \, dA \quad \text{or} \quad \int_{0_1}^{0_2} P' dA \,, \quad . \quad . \quad . \quad . \quad . \quad . \quad . \quad . \quad (18)$$

where A is the area of the section whose radius is r and 0_1 and 0_2 denote the values of A at the extremities of the major axis. This is a convenient form for reducing the experimental results.

In the theoretical case we have one convenient check of the somewhat laborious reduction which gave us the expressions for the pressures.

It is shown in LAMB's 'Hydrodynamics'* that the kinetic energy of the fluid due to the motion of a body through it in one plane may be written in the form

$$2T = Au^2 + Bv^2 + R\,\Omega^2 + 2F\,v\,\Omega,$$

A, B, F and R depending on the configuration of the body. The components of the resultant fluid force and couple on the body are

$$-X = \frac{d}{dt}\cdot\frac{\partial T}{\partial u} - \Omega\frac{\partial T}{\partial v}, \qquad -Y = \frac{d}{dt}\cdot\frac{\partial T}{\partial v} + \Omega\frac{\partial T}{\partial u}, \qquad -N = \frac{d}{dt}\frac{\partial T}{\partial \Omega} - v\frac{\partial T}{\partial u} + u\frac{\partial T}{\partial v},$$

giving in this case (steady motion, *i.e.*, $\dot{v}$ and $\dot{r} = 0$) $-X = -\Omega Bv$; in the case of the spheroid $F = 0$ (LAMB, *loc. cit.*, p. 162) and B is the mM of the present paper, where m is the mass of fluid displaced by the spheroid.

Evaluating the integral $\int P' dA$, we obtain the above value for X.

11. *Resultant Lateral Pressures, Lateral Force and Yawing Moment.*—The component of the pressure p in the plane xOy is $p \cos \omega$. The resultant pressure on the section perpendicular to xOy, through a point whose eccentric angle is ψ, is

$$P'' = b \sin \psi \int_0^{2\pi} p \cos \omega \, d\omega,$$

acting normal to the generator in the plane of xy

$$P'' = b \sin \psi \int_{-1}^{+1} p \,.\, d(\sin \omega) = \int_{-z_0}^{+z_0} p \,.\, dz, \quad . \quad . \quad . \quad . \quad . \quad . \quad (19)$$

z_0 being the radius of the section ($= b \sin \psi$).

* 3rd Edition, Chapter VI.

The resultant lateral force is

$$\int_{s_1}^{s_2} \mathrm{P}'' \sin\theta \,.\, ds$$

$$= \int_{-a}^{a} \mathrm{P}'' \,.\, dx. \quad . \quad . \quad . \quad . \quad . \quad . \quad . \quad . \quad . \quad . \quad . \quad . \quad (20)$$

12. The yawing moment about the axis of z is $\int \mathrm{P}'' l \,.\, ds$, where l is the perpendicular distance between the z axis and the line of action of P″ or the normal at the point ψ in the plane xOy.

$$l = \frac{(a^2 - b^2)\sin\psi\cos\psi}{\sqrt{a^2\sin^2\psi + b^2\cos^2\psi}}, \quad \frac{ds}{d\psi} = \frac{\sqrt{dx^2 + dy^2}}{d\psi} = \sqrt{a^2\sin^2\psi + b^2\cos^2\psi},$$

therefore the yawing moment is

$$\int \mathrm{P}'' (a^2 - b^2)\sin\psi\cos\psi \,.\, d\psi. \quad . \quad . \quad . \quad . \quad . \quad . \quad . \quad . \quad . \quad (21)$$

$$= -\int \mathrm{P}'' a^2 \cos\psi \, d(\cos\psi) - \int \mathrm{P}'' b^2 \sin\psi \, d(\sin\psi)$$

$$= -\tfrac{1}{2}\int \mathrm{P}'' \, d(x^2 + y^2). \quad . \quad . \quad . \quad . \quad . \quad . \quad . \quad . \quad . \quad . \quad . \quad . \quad (22)$$

As in the case of (18) for longitudinal force, (20) and (22) are convenient for reducing the experimental results.

13. On integrating the expressions for p, given in (9), we find that theoretically

$$\frac{\mathrm{P}''}{\frac{1}{2}\rho\mathrm{V}^2} = \frac{2\pi ab^2 \,.\, \cos\beta}{a^2\sin^2\psi + b^2\cos^2\psi} \sin^2\psi \Big[(1 + \mathrm{L})(1 + \mathrm{M})\cos\psi\sin\beta$$

$$- (1 + \mathrm{L})(1 + e^2\mathrm{N}\cos 2\psi)\frac{a}{\mathrm{R}} + (a^2\sin^2\psi + b^2\cos^2\psi)\frac{1}{a\mathrm{R}}\Big]. \quad (23)$$

This expression again provides a check on the reductions, since the resultant lateral force $\mathrm{Y} = \mathrm{A}ur$ and the yawing moment

$$\mathrm{N} = (\mathrm{B} - \mathrm{A})uv,$$

A being mL of the present paper.

II. Method and Range of Experiments.

(a) *Measurement of the Pressures in rectilinear Motion.*

14. The experiments were conducted in a 4-foot wind tunnel at a wind speed of 40 feet per second. Previous experiments had shown that over the forward half of the model there was no consistent "speed effect"; hence it was not considered necessary to

include measurements at different wind speeds in the investigation, particularly as interest was centred mainly on the forward half of the spheroid.

The model used was made of wood, and was 2 feet long, the minor axis being 6 inches ($a/b = 4$). It was supported in the wind tunnel by means of a steel spindle ($\frac{5}{16}$-inch diameter) placed in the chuck of the aerodynamic balance. It was thus easy to vary the angle of incidence (β). A length of soft composition tubing was embedded in the model in the usual way, flush with the surface: the tube was placed in a plane through the major axis. One end of the tube was sealed and the other connected to a manometer. A series of holes were bored in the tube at suitable positions, all the holes except one being sealed in any one experiment: the normal pressure at the position occupied by the hole left open could then be observed on the manometer. The inclination (ω) to the horizontal of the plane containing the tube could be varied in the following manner: The upper end of the supporting spindle was attached to a circular graduated band embedded in the model (flush with the surface), in the central plane perpendicular to the major axis. After slackening a nut it was possible to rotate the entire spheroid about the major axis and set the tube at any desired angle to a horizontal plane. Observations were taken at the following values of β:—

0, 2, 4, 6, 10 and 20 degrees,

and of ω:—

0 to 180° at intervals of 15°.

The results, specimens of which are plotted in the drawings appended, are given as coefficients ($p/\frac{1}{2}\rho V^2$), and have been corrected for the variation of static pressure in the channel.*

From the distribution of normal pressures the average pressures over a number of sections perpendicular to the major axis have been calculated (see § 21), and also the distribution of resultant lateral pressure per foot run (§ 22). From the former we can calculate by integration the "form resistance," from the latter the lateral force and yawing moment due to normal pressures. For comparison with these results obtained by integration, the actual drag, lateral force, and yawing moments were measured on the aerodynamic balance. The drag at zero yaw was determined with the model supported on wires; for measuring the other quantities the model was supported on a spindle, the necessary corrections being applied for the effect of the spindle.

(*b*) *Measurements of the Pressures on a Spheroid spinning about a Minor Axis.*

15. As in the previous case, a length of composition tubing was inserted in the spheroid, but in view of the fact that in these experiments the model was moving relative to the earth, a special seal had to be constructed to transmit the pressures to the manometer.

* "Experiments in a Wind Channel on Elongated Bodies of approximately Streamline Form. Part I." Pannell, Jones and Pell, 'Rep. and Mem., 564, Aeronautical Research Committee.'

The model was supported, with the major axis horizontal, in a strong graduated band (A) (fig. 2), made in two pieces, and such that by slackening two screws the model could be rotated about the major axis, so that the angle between the plane containing the tube and the horizontal could be varied. The upper half of the band was attached by means

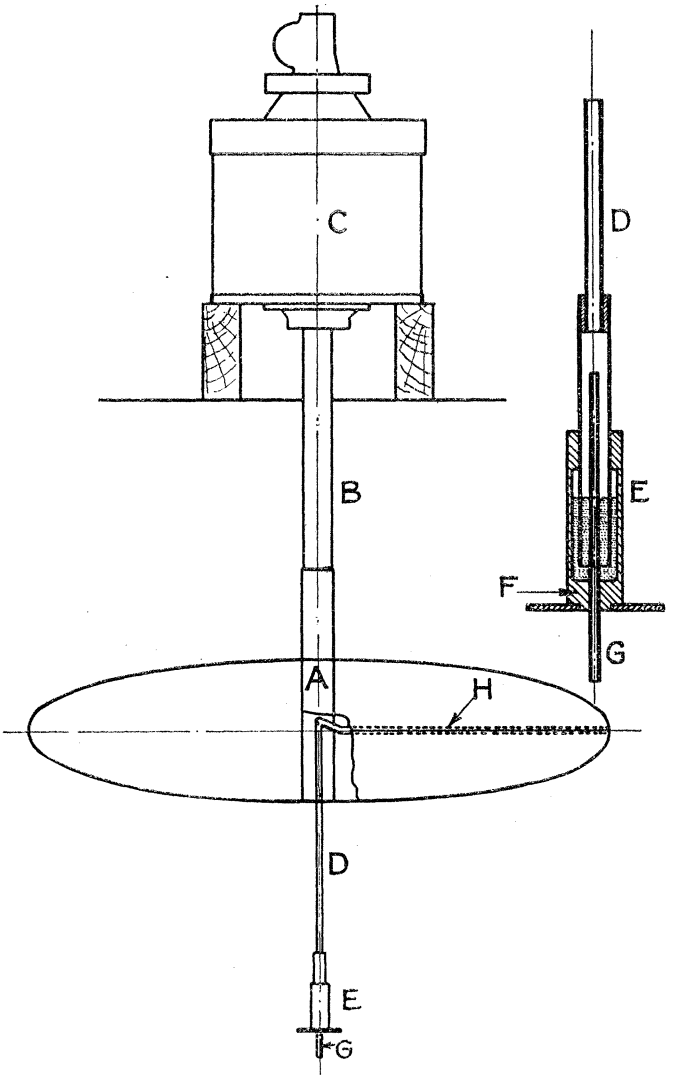

FIG. 2.—Arrangement of Apparatus for Spinning Motion.

A. Graduated Band.
B. Supporting Spindle.
C. Electric Motor.
D. Tube.
E. } Mercury Seal.
F. }
G. Tube to Manometer.
H. Composition Tubing.

of a substantial spindle (B) to the shaft of the electric motor (C), which in turn was carried on a strong wooden structure placed across the room in which the experiments were conducted.

A tube (D) about $\frac{1}{4}$-inch in diameter passed through the lower half of the band, the upper end terminating in the interior of the model, which was hollow. The open end of the composition tubing was connected to this end of D by means of a piece of rubber tubing of a sufficient length to enable the spheroid to be rotated through 180 degrees about the major axis without causing a stoppage in the tube. The lower end of the tube D terminated in a mercury seal (E), the body (F) of which was clamped to a rigid stand so that the centre was vertically below the centre of the spheroid or the centre of the electric motor. The tube (G) leading from the mercury seal was connected to the manometer.

In order to ensure a steady speed of rotation, power was supplied to the motor from accumulators, the wiring being such that by a suitable arrangement of switches a voltage of 4, 6, 8, 10 or 14 could be used, and thus the speed of the motor varied without inserting resistances in the armature circuit. This speed was measured by means of a counter geared to the motor shaft.

Observations of the temperature of the air in the room, and also barometric pressures, had to be taken in these experiments (where the absolute velocity of the spheroid was needed), in order to ascertain the value of ρ : in wind-tunnel experiments the observed "speed" is a direct measure of ρV^2, since the speed is observed on the usual Chattock manometer. The results (which are given as coefficients of the form $p/\frac{1}{2}\rho a^2\Omega^2$, where Ω is the angular velocity of the spheroid and a the semi-major axis) have been corrected for variations in ρ. Further, the observations give the normal pressure at any point plus the (negative) pressure caused by the action of centrifugal force on the air in the rotating tube. Corrections have been applied to allow for this, and the results, which are represented graphically in the drawings appended, show the actual normal pressure coefficient. It should be borne in mind that it was not always possible to repeat any particular speed accurately : the speeds given on the curves are means of the observed speeds, but in calculating the coefficients the actual speeds have, of course, been used.

(*c*) *Measurements of the Pressures on a Spheroid turning about an Axis parallel to a Minor Axis.*

16. These experiments were conducted on the whirling arm, which has been described elsewhere.* The major axis of the spheroid was horizontal throughout the experiments, and its centre moved in a circle of 27·96 feet radius. Fig. 3 shows the method of supporting the model, side and end views being given. In some preliminary experiments the model was held in place by means of a vertical spindle supporting a circular band flush with the model, as in case (*b*). It was found, however, that to make the support rigid the spindle had to be of such a diameter that the interference was

* "Airscrews in Theory and Experiment," FAGE, Ch. V, and the Reports of the Advisory Committee for Aeronautics.

appreciable. In case (*b*), where the spindle did not move parallel to itself, the interference could be ignored. By supporting the model from the after-end no appreciable interference could be observed on the forward half of the spheroid.

As in case (*a*), provision was made for rotating the model about its major axis, one length of composition tubing being again sufficient for investigating the entire surface of the spheroid. The after-end of the model was made of metal and graduated, a pointer being attached to the horizontal member of the supporting structure. Moreover, the entire supporting structure was attached to a turn-table rigidly fixed to the whirling arm, and the centre of the turntable was vertically above the centre of the spheroid; it was thus possible to vary the angle of yaw without altering the radius.

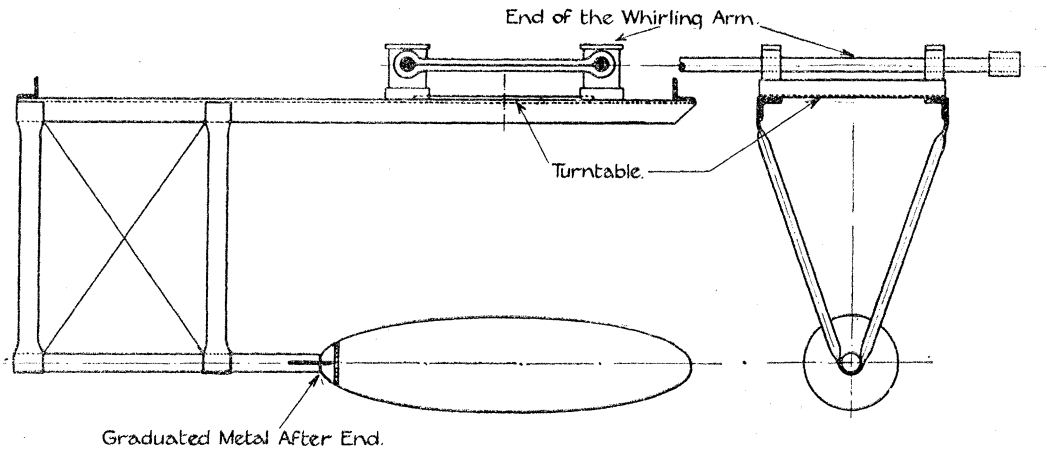

FIG. 3.

17. The speed of the spheroid over the ground was observed by counting the revolutions of the whirling arm, a make and break in a bell circuit being arranged to ring the bell once in each revolution. Owing to the swirl caused by the movement of the arm, the velocity of the spheroid through the air is less than that over the ground, and hence the swirl had to be measured. This was done by means of a pitot tube fixed at the end of the arm opposite to that at which the model was supported. The gauge reading gave $\frac{1}{2}\rho V^2$, where V is the speed through the air, plus a negative pressure of $\frac{1}{2}\rho V_1^2$, where V_1 is the speed over the ground, the latter component being due to the action of centrifugal force of the air in the tube transmitting the pressure from the pitot to the manometer. A previous investigation shows that, at the speeds used, the effects of compressibility are negligible. The tube was laid along the arm, and was connected to the manometer through a double mercury seal placed at the upper end of the central shaft. As in the spinning experiment, it was necessary to take observations of temperature and barometric pressure in order to determine ρ. The temperature variations in this case were of some importance owing to seasonal effects, which were accentuated by the fact that the arm is housed in a corrugated iron building. It was found, after a complete investigation

with and without the spheroid in position, that the speed of the arm through the air was approximately 7 per cent. less than the speed over the ground.

18. After the swirl had been determined, the pitot was disconnected, and the composition tubing on the spheroid connected to the seal in readiness for taking observations of the pressures. Now the normal pressure cannot exceed $\frac{1}{2}\rho v^2$ at any point of the model (where v is the velocity of that point through the air), and the pressure drops rapidly away from the point of maximum pressure and is small in comparison with $\frac{1}{2}\rho v^2$ over the greater part of the model. It is obvious, therefore, that if one side of the manometer be open to atmosphere, the other being connected to the spheroid, the greater part of the reading on the manometer will be due to the centrifugal force (on the air in that part of the connecting tubes which turns with the arm) giving rise to a suction equal to $\frac{1}{2}\rho v_1^2$, where v_1 is the actual speed of the point under consideration. Moreover, since v_1 is greater than v, owing to swirl, the centrifugal pressure will always be greater than the aerodynamic normal pressure, and in the great majority of cases much greater. It was therefore considered advisable to connect the open end of the manometer to a static pressure tube moving with the spheroid. Experiments were conducted to determine the best position for the static pressure tube, and ultimately one was fitted up in front of the spheroid at the same radius as the centre of the spheroid, and well above the axis, to avoid interference. The reading with this tube connected to one side of the manometer and the other side open to the atmosphere was very approximately $\frac{1}{2}\rho v_2^2$, where v_2 is the speed of the static pressure tube over the ground. The apparatus was so arranged that, by means of glass cocks suitably placed, the manometer could be connected at will to—

(i) The static pressure tube and spheroid.
(ii) The static pressure tube and atmosphere.

Check readings of (ii) were frequently taken, particularly when the orientation of the spheroid was altered. The static pressure reading, however, did not vary as the spheroid was moved.

19. Again, it is obvious from the nature of the motion that v is not constant for every point on the spheroid. For example, if the nose of the spheroid points inwards, as in the case of an airship in curvilinear flight, the radius of the circle described by the forward end of the major axis is less than that of the circle described by the after-end. Hence v_1 also varies, so that the centrifugal pressure of the air in the tube on the model is not quite balanced by the centrifugal pressure of the air in the tube connected to the static pressure tube, and a correction has to be applied. The results, as presented, include (*a*) this correction, (*b*) the density correction, (*c*) a correction arising from the fact that the static pressure reading was not accurately $\frac{1}{2}\rho v_2^2$, and (*d*) the swirl correction. The pressures given represent the normal pressure divided by $\frac{1}{2}\rho V^2$, where V is the speed of the centre of the spheroid, and is constant for all attitudes of the spheroid when the angular velocity of the arm is constant. It should be noted, however, that as in § 15

it was not possible to repeat accurately any particular speed : the speed quoted is, therefore, the mean of a number, each of which approximates very closely to the mean. The actual speed has, of course, been used in calculating the coefficients. Further, in view of the fact that the pressures have been divided by V^2 and not by v^2, there are a few points where the pressure coefficient exceeds unity.

20. The method of procedure may be expressed symbolically as follows :—

p is the pressure at a point P.
V and v the speeds through the air of the centre and of P respectively.
V_1 and v_1 the speeds over the ground of the centre and of P respectively.
$V_1 = v_2$ the speed of the static pressure tube over the ground.
V_1 and $v_1 = R\Omega$ and $R'\Omega$ respectively (Ω the angular velocity).
G_1 and G_2 are respectively the readings of the manometer when connected to

(1) Spheroid and static pressure tube.
(2) Atmosphere and static pressure tube.

We have said that G_2 was not accurately $\frac{1}{2}\rho v_2^2$.
Let $G_2 = \frac{1}{2}\rho v_2^2 - p_s$,

$$G_1 = (p - \tfrac{1}{2}\rho v_1^2) - (p_s - \tfrac{1}{2}\rho v_2^2) = p - p_s + \tfrac{1}{2}\rho (v_2^2 - v_1^2) = p - p_s + \tfrac{1}{2}\rho V_1^2\left(1 - \frac{v_1^2}{V_1^2}\right)$$

$$\frac{G_1}{\frac{1}{2}\rho V^2} = \frac{V_1^2}{V^2}\left\{\frac{p}{\frac{1}{2}\rho V_1^2} - \frac{p_s}{\frac{1}{2}\rho V_1^2} + \left(1 - \frac{R'^2}{R^2}\right)\right\},$$

and R′ is easily calculable from the geometry of the system.

III. Discussion of Results.

(a) *Rectilinear Motion—Comparison between Theory and Experiment.*

21. As stated above (§ 14), a few cases have been selected for diagrammatic presentation of the results in order that the nature of the comparison between the theoretical and experimental results may be seen at a glance. Referring first of all to figs. 4, 5, 6 and 7, in fig. 4 the pressure coefficients have been plotted against angle of roll (or ω) for four sections $x = \text{const.}$ The values of x shown are 0·896, 0·837, 0·727 and 0·590. The experimental curves have been given for the following values of β : 0, 2, 4, 6, 10 and 20 degrees : to avoid congestion, theoretical curves have been given for only two values of β (10° and 20°).

It will be seen that the theoretical results agree remarkably well for the given range of x with those obtained by experiment. It may be stated here that the agreement is, in

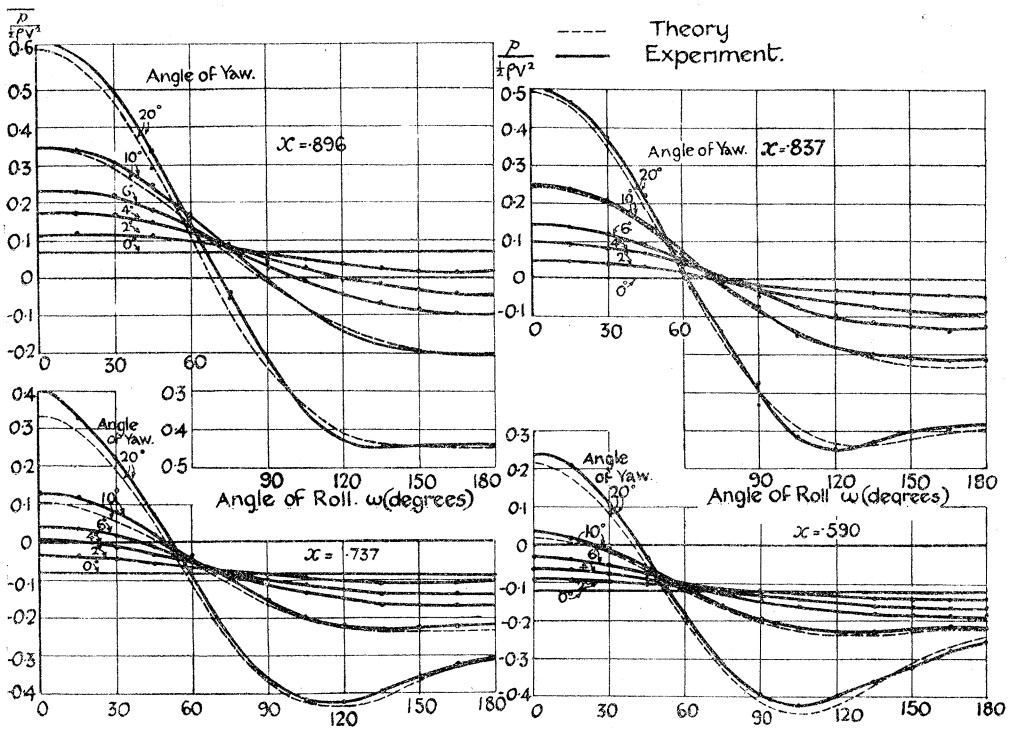

FIG. 4.—Rectilinear Motion—Pressures.

general, equally good for all values of x included in the range $1 > x > 0$ (the forward end of the spheroid), and also for all negative values of x up to a certain point. This point varies with β and ω, as may be seen on reference to figs. 5 and 6. In these diagrams $p/\frac{1}{2}\rho V^2$ has been plotted against x for certain values of β and ω. In fig. 5, $\beta = -20°$.

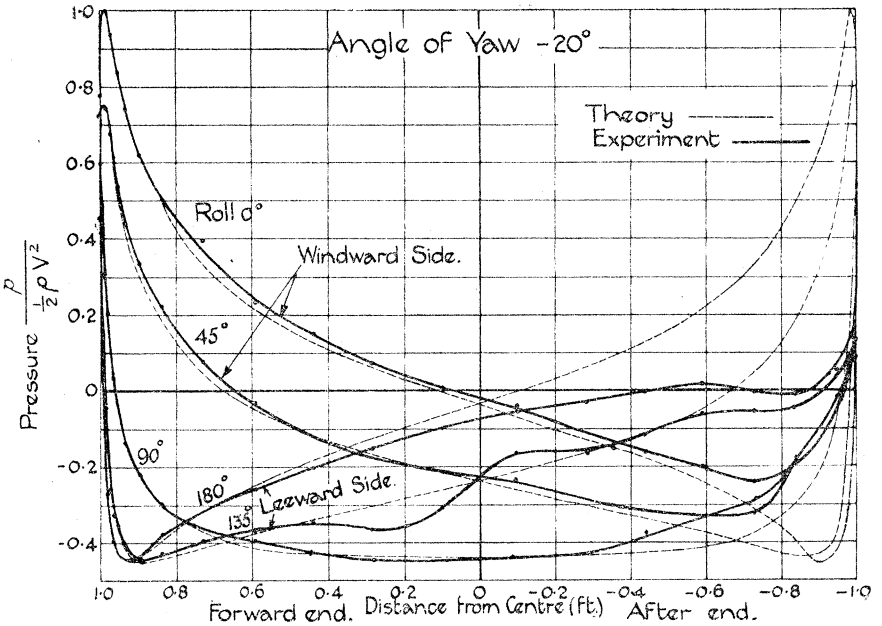

FIG. 5.—Rectilinear Motion—Pressures.

When $\omega = 90°$ agreement is good within the range $1 > x > -0{\cdot}3$; the same holds good for $\omega = 0°$ and $45°$ (*i.e.*, on the windward side of the model). Agreement is not so good on the leeward side, but even in that case it may be regarded as satisfactory on the forward half of the model. In fig. 6 ($\beta = -10°$) the theoretical and experimental

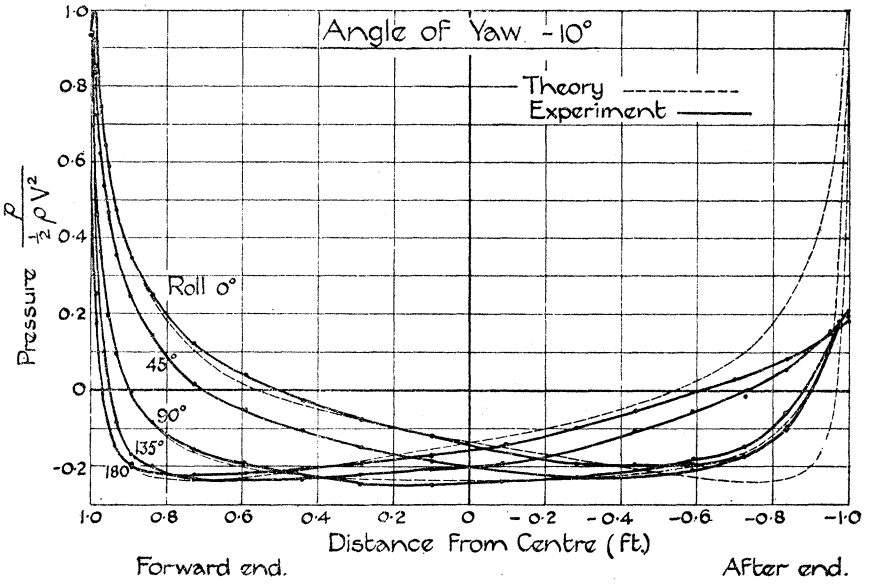

FIG. 6.—Rectilinear Motion—Pressures.

curves are nearly coincident for three-quarters of the length of the model, or even more, except on the equator on the leeward side. For the case of $\beta = 0$ reference should be made to fig. 7, giving the average pressures. In this case the pressures are independent of ω by symmetry, and good agreement obtains along $0{\cdot}95$ of the length of the model.

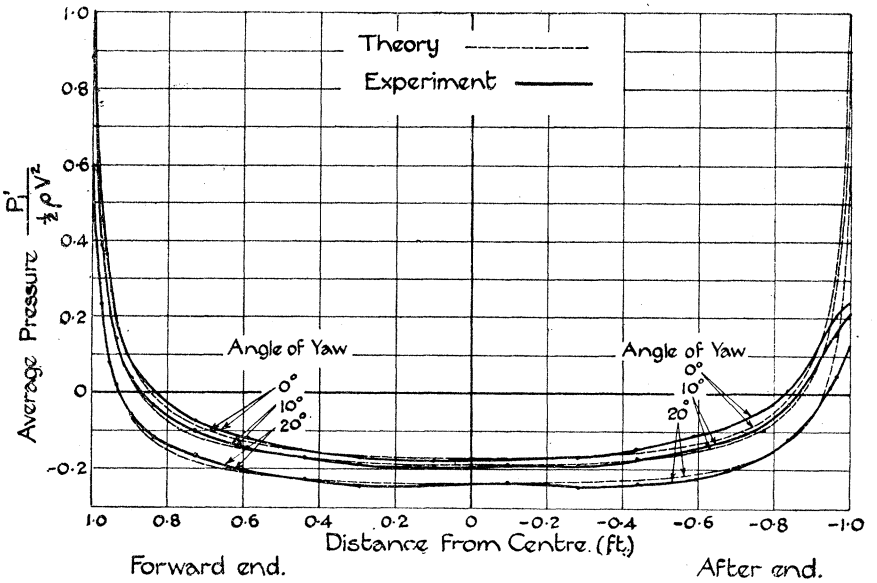

FIG. 7.—Rectilinear Motion—Average Pressures.

A glance at the curves for $\beta = 10°$ and $\beta = 20°$ shows that the same is true for the *average* pressures in these cases. This result is rather surprising for $\beta = 20°$, since the actual pressures are not in such good agreement on the after half of the model.

22. Fig. 8 gives the distribution of the resultant lateral pressures per unit run—*i.e.*, the resultant pressure in the equatorial plane (xOy) normal to the surface. In this case

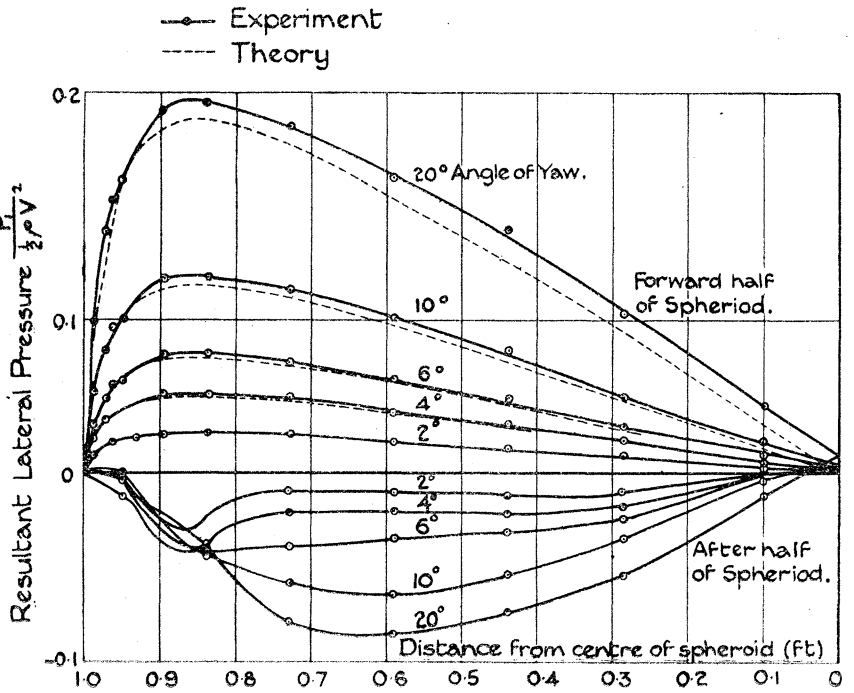

FIG. 8.—Rectilinear Motion—Resultant Lateral Pressures.

also, agreement is good on the forward half of the model, but over the after-half the $\beta = 20°$ curves are not so close to one another. The remaining curves ($\beta = 2°$, $4°$, $6°$ and $10°$) follow one another more closely up to $x = -0{\cdot}5$ approximately.

An integration of the experimental curves, shown in fig. 7, gives the longitudinal force (acting along the x axis) due to the normal pressure. The following table gives the results obtained and the actual total longitudinal force measured on the balance. The wind speed is 40 ft./sec.

β degrees.	Longitudinal force (lbs.).		Ratio $\frac{\text{integrated}}{\text{measured}}$.
	Measured.	Obtained by integration.	
0	—0·0211	—0·0085	0·40
6	—0·0229	—0·0096	0·42
10	—0·0231	—0·0104	0·45
20	—0·0236	—0·0115	0·49

It will be seen that the normal pressures account for between 40 and 50 per cent. of the drag of the spheroid, the remainder being, presumably, due to skin friction.

An integration of the experimental curves of fig. 8 will give the lateral force on the model, and an integration of the same ordinates plotted against $x^2 + y^2$ will give twice the yawing moment. The following tables give the results obtained and also those derived from measurements on the aerodynamic balance.

β degrees.	Lateral force at 40 ft./sec. (lbs.).		Ratio A/B.
	(A) As measured on the balance.	(B) As obtained by integration.	
0	0	0	—
4	0·0155	0·0123	1·26
6	0·0267	0·0225	1·19
10	0·0564	0·0454	1·24
20	0·151	0·127	1·19
Moments about a minor axis (lbs. ft.).			
0	0	0	—
2	0·023	0·026	0·89
4	0·045	0·052	0·87
6	0·067	0·077	0·87
10	0·106	0·122	0·87
20	0·179	0·207	0·86

The measured lateral force is greater than that obtained by integrating the pressures, but the reverse is true in the case of the yawing moment.

(*b*) *Spinning Motion—Comparison between Theory and Experiment.*

23. From the expression 9 of § 5, it is obvious that theoretically the pressures are the same on the windward part of the spheroid as on the leeward. We need in this case only consider the terms in Ω^2 in this expression, and these terms involve only $\cos^2\omega$ and $\sin^2\omega$, so that the pressure is the same at ω, $\pi - \omega$, $\pi + \omega$ and $2\pi - \omega$. The results are reproduced graphically in fig. 9, where the pressures divided by $\frac{1}{2}\rho a^2\Omega^2$ have been plotted along the length of the spheroid for two quadrants. In this figure are also plotted the corresponding experimental results. From symmetry, the pressures on the first and fourth quadrants facing the relative wind ($90° \geqslant \omega \geqslant -90°$) of one half ($0 < \psi < 90°$) of the spheroid are the same as the pressures on the other two quadrants ($90° \leqslant \omega \leqslant 270°$) of the other half of the spheroid ($90° < \psi < 180°$) (also facing the relative wind). The pressures obtained at the highest speed of rotation are shown. We note from this diagram

that the agreement between theory and experiment is not good at the extreme ends of the model. On the equator agreement becomes good on the windward side at a distance from the end of less than a fortieth of the length of the model, and remains good until after the middle is passed, when theory and experiment again diverge. This is natural,

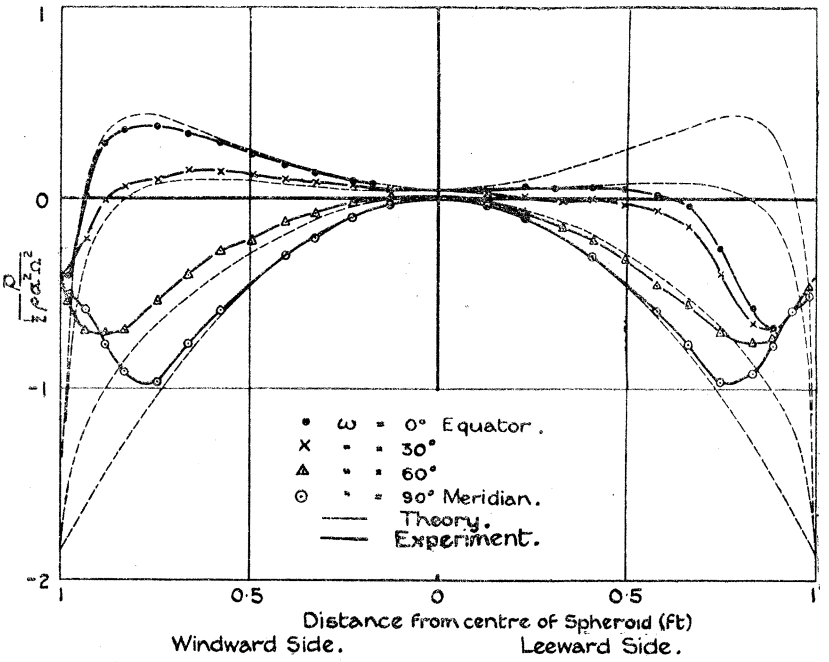

Fig. 9.—Spinning Motion—Pressures.

since we are now on the leeward side, and discrepancies might be expected. On the meridian section agreement does not become good until we are about one-eighth of the length of the model from the end, and the experimental pressures are, as was to be expected, symmetrical at both ends of the model along this generator. Along generators intermediate between the equator and the meridian, the distance from the end at which good agreement commences decreases as we approach the equator, but agreement on the leeward side becomes less good.

24. In figs. 10 and 11 the pressures are plotted against ω for each of the four mean speeds of rotation. In some cases the theoretical curve is also drawn. No useful object would be gained by adding the theoretical curves at values of x near the extremities of the spheroid, since the agreement is not good (see fig. 9). An examination of the curves shows that there is an appreciable and, on the whole, very consistent speed effect. One interesting characteristic of the speed effect is that as the angular velocity increases the curves become more symmetrical with reference to $\omega = \pi/2$—*i.e.*, the pressures on the leeward and windward sides become more alike. Moreover, we note that at the same time the experimental curves approach the theoretical curves as the speed becomes

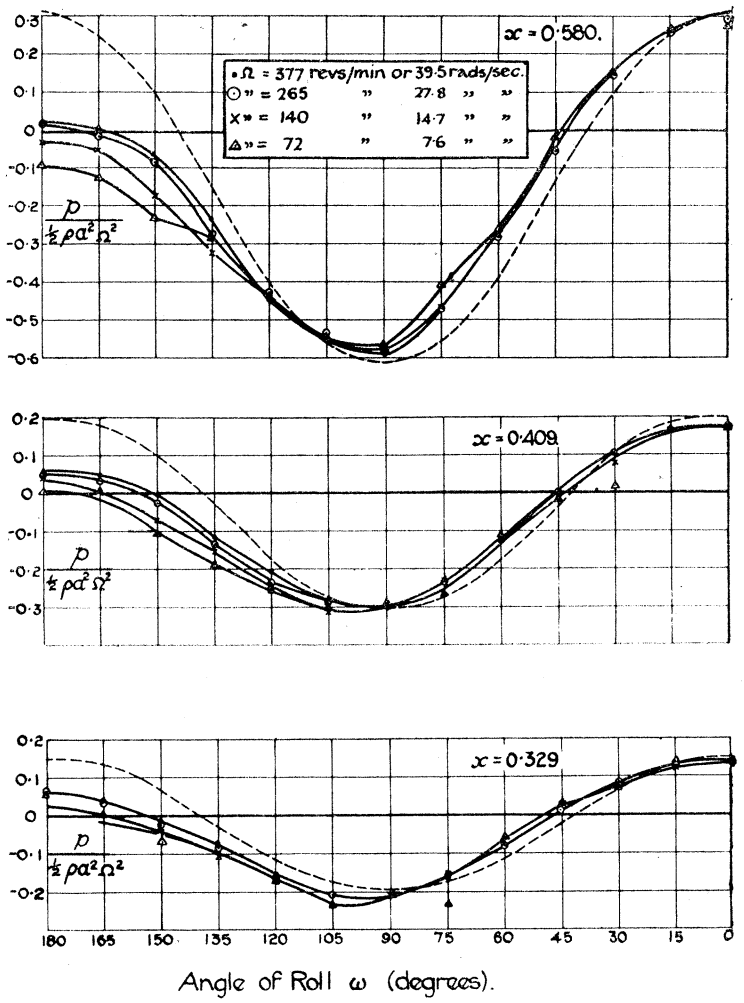

FIG. 10.—Spinning Motion—Pressures.
- - - - - - Theory. ——— Experiment.

greater. From a purely academical point of view it would have been of great interest to have taken readings at a higher speed, but at higher speeds undesirable vibrations were set up in the structure available for supporting the model and motor.

25. Fig. 12 shows the average pressure along one-half of the spheroid. This figure confirms the remarks on speed effect, except between $x = 0{\cdot}75$ and $0{\cdot}85$. In that region the average pressure at the lowest speed approaches the theoretical more closely, but it will be seen that the curve giving the average pressure at the two highest speeds intersect nearer the theoretical curve than do the experimental curves at the second and third or third and fourth speeds. This indicates that if the speed were increased beyond the highest used in the experiment, the resulting average pressures would be in better agreement with the theoretical.

This conclusion is further confirmed by fig. 13, which shows the resultant lateral pressure distribution normal to the surface. The curves are symmetrical with respect

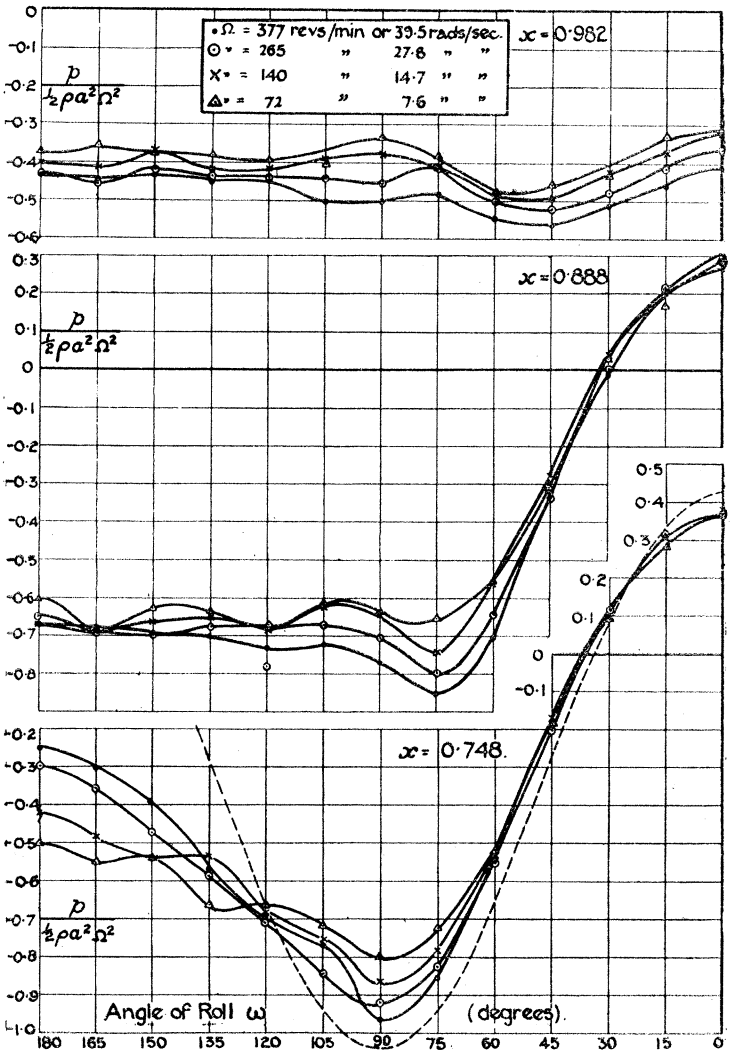

FIG. 11.—Spinning Motion—Pressures.
- - - - - - Theory. ——— Experiment.

to the origin—*i.e.*, the resultant pressures are negative when x is negative, giving, of course, a zero lateral force on the complete spheroid. A calculation of the yawing moment about the z axis, due to the normal pressures on one-half of the spheroid, shows that the line of action of the lateral force on the hemispheroid passes through a point 0·61 to 0·64 foot from the centre. The following table gives the lateral force and yawing moment on the hemispheroid:—

Ω (rads./sec.).	$\frac{\text{Lateral force}}{\frac{1}{2}\rho a^2\Omega^2}$.	$\frac{\text{Yawing moment}}{\frac{1}{2}\rho a^2\Omega}$.	$\frac{\text{Moment}}{\text{Force}}$.
39·5	0·0621	0·0392	0·636
27·8	0·0695	0·0429	0·618
14·7	0·0785	0·0484	0·615
7·6	0·0822	0·0500	0·609

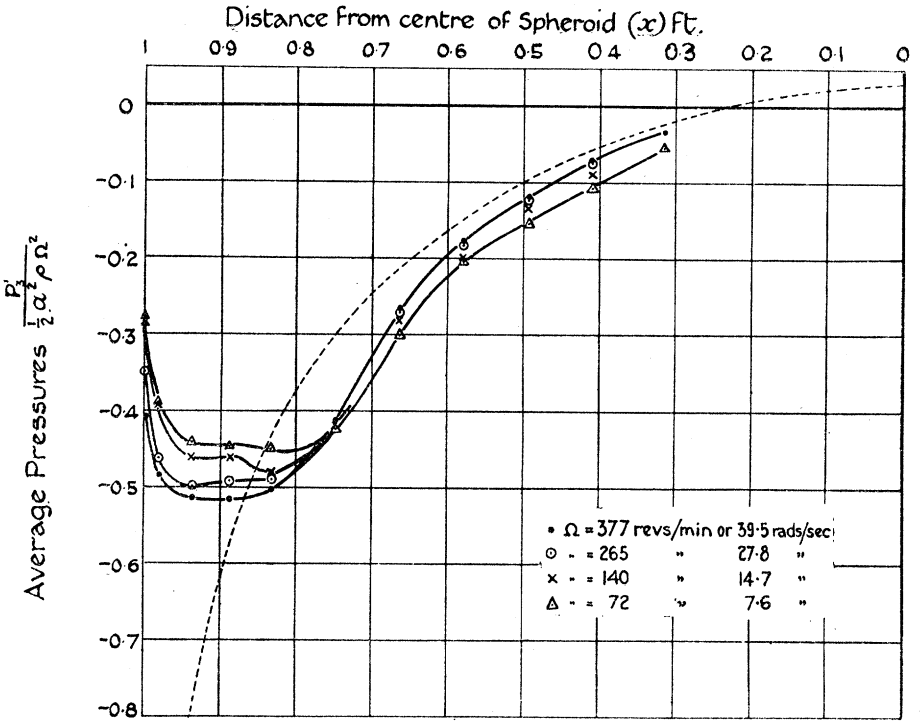

FIG. 12.—Spinning Motion—Average Pressures.
- - - - - - Theory. ——— Experiment.

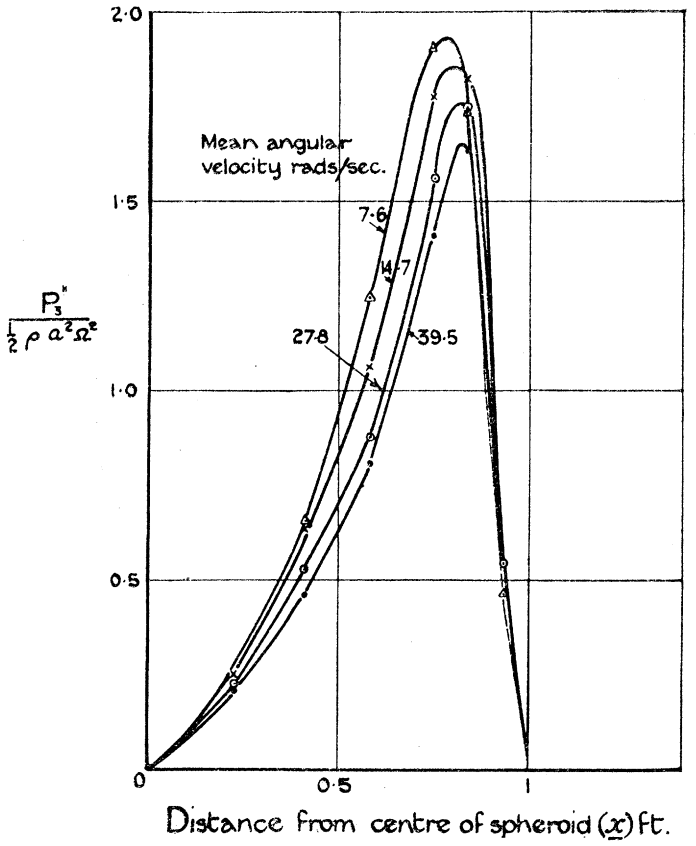

FIG. 13.—Spinning Motion—Resultant Lateral Pressures.

(*c*) *Curvilinear Motion—Comparison between Theory and Experiment, and between Rectilinear and Curvilinear Motion.*

26. As in the two previous cases, a selection of the results has been made for the purpose of graphical representation. To plot all the observations at all speeds would mean the inclusion of a large number of drawings unless clearness were sacrificed. The illustrative cases chosen in figs. 14 and 15 are the distribution of pressure along the

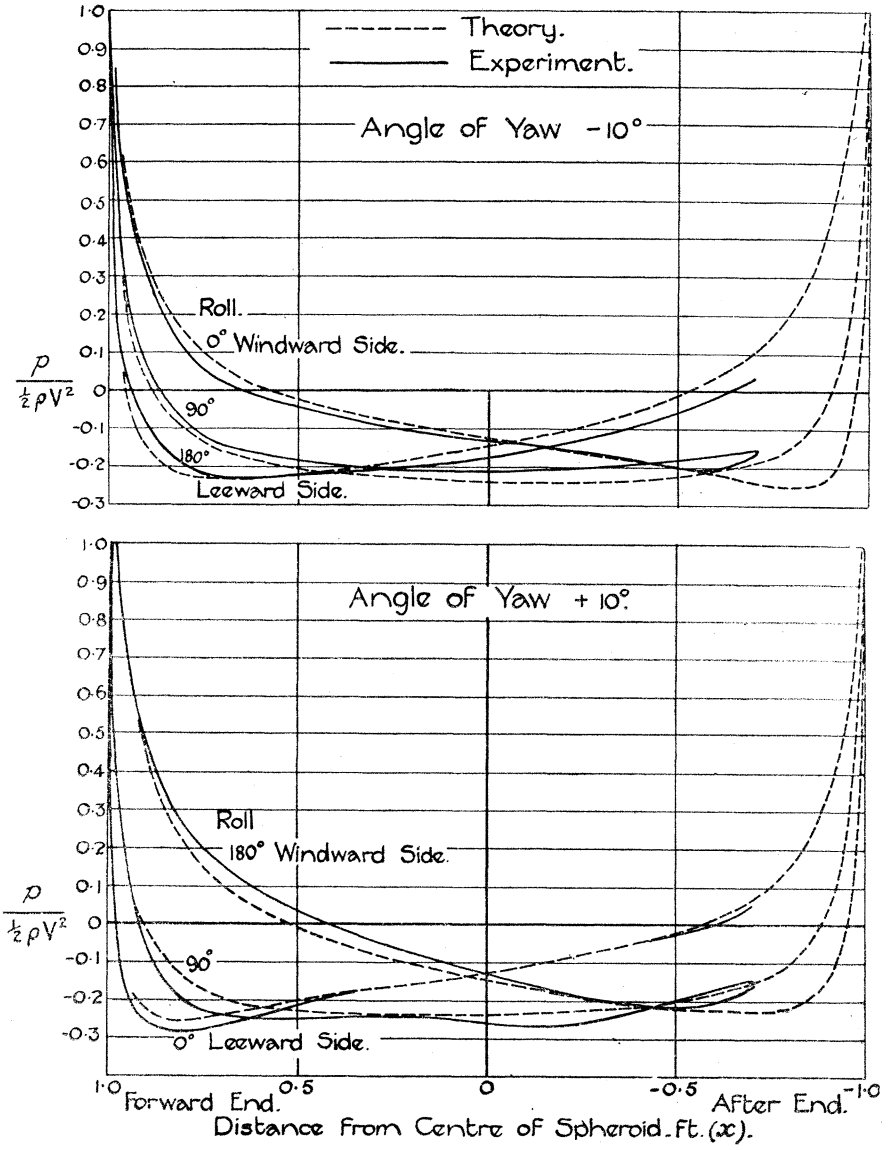

FIG. 14.—Curvilinear Motion—Pressures.

generators $\omega = 0°$ and $180°$ (the equator) and $\omega = 90°$, at angles of yaw of $\pm 10°$ and $\pm 20°$, the radius of the turning circle being $-27{\cdot}96$ feet. Owing to the method of supporting the model, it was not possible to extend the range of observations to the extreme after-end of the model, and seeing that under no circumstances could agreement be expected

at the after-end, it was not considered worth while to use another method of support. The agreement between theory and experiment may be regarded as good, though perhaps not so good as in the case of rectilinear motion. Either fig. 14 or fig. 15 shows that near the

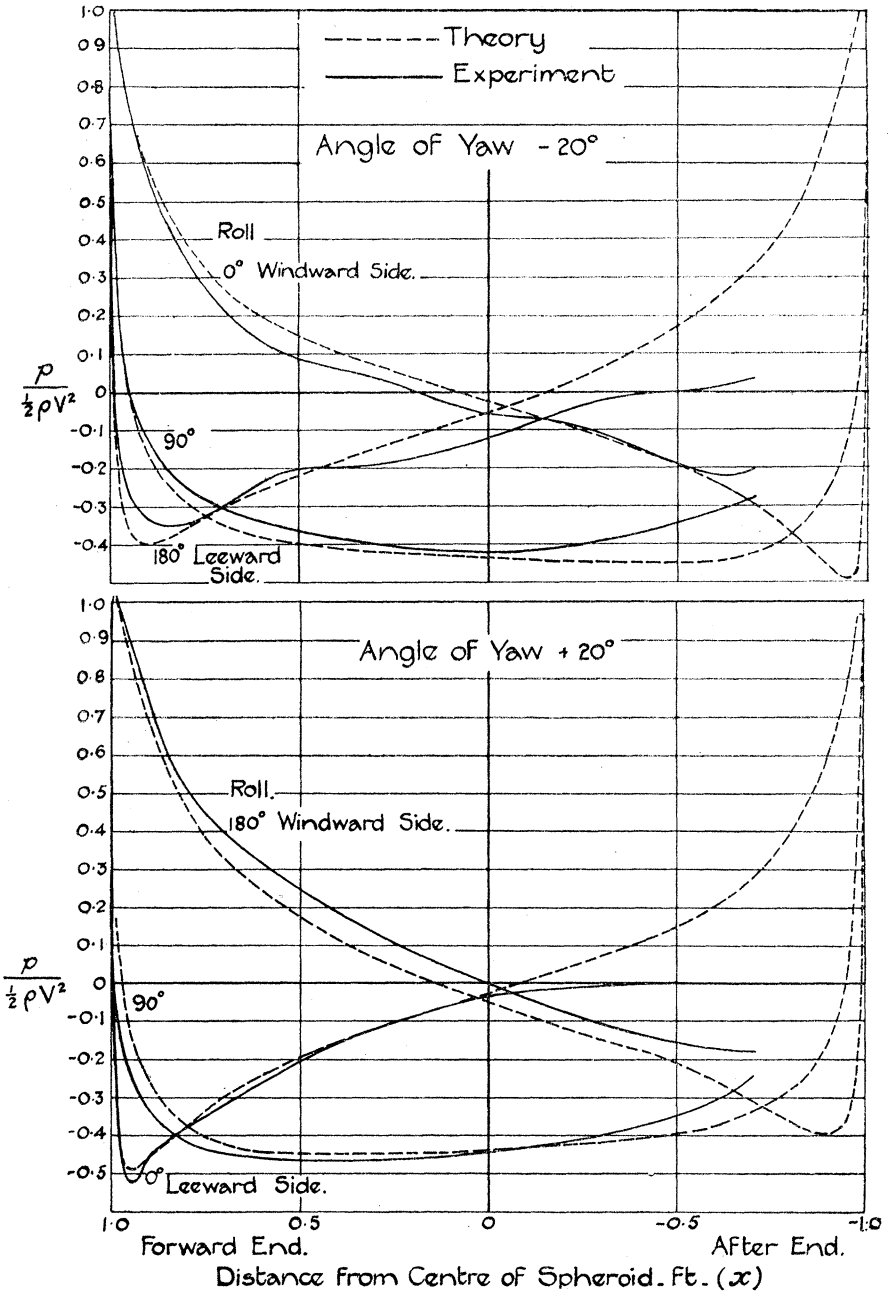

FIG. 15.—Curvilinear Motion—Pressures.

forward end on the windward side of the equator the theoretical pressure is less or greater than the observed, according as the angle of yaw is positive or negative. The

reverse is the case at $\omega = 90°$ and on the leeward side of the equator. This indicates that the effect of rotation is really greater than theory would lead one to expect. In order to demonstrate this more clearly, the curves of figs. 6 and 14 have been re-plotted in figs. 16 and 17. The experimental curves in rectilinear and curvilinear motion are given together, and similarly the theoretical curves for — 10° yaw. It is at

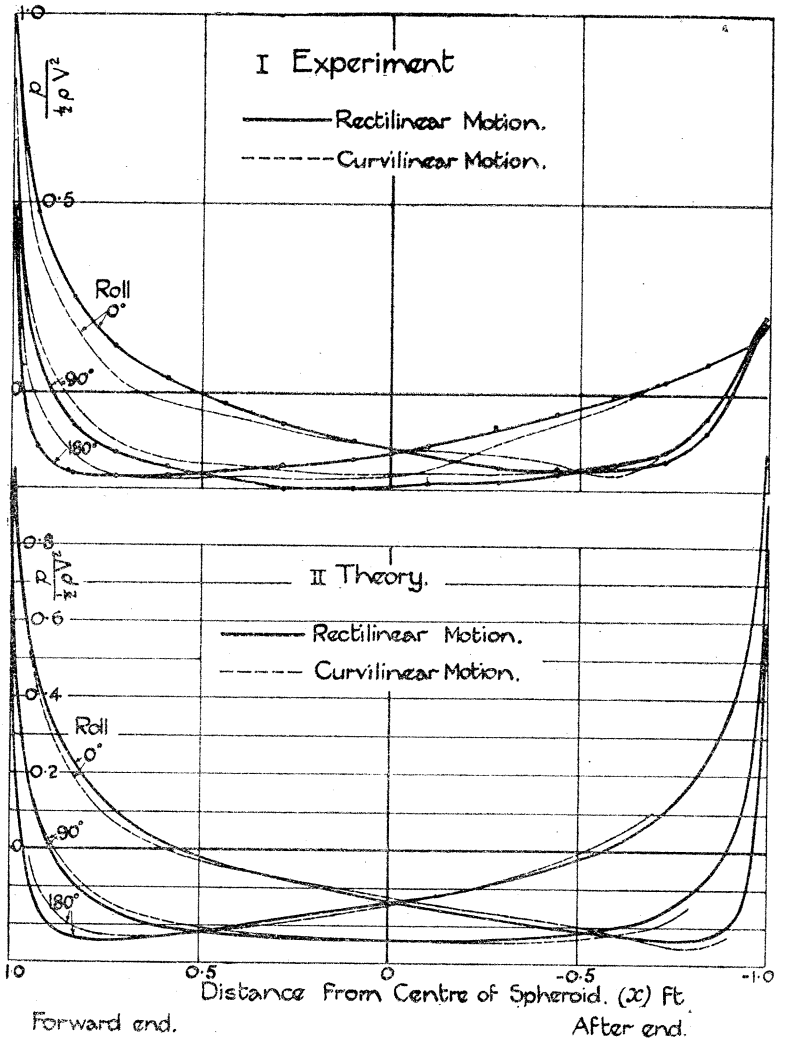

FIG. 16.—Comparison between Rectilinear and Curvilinear Motion. Angle of Yaw —10°.

once obvious that the effect of rotation is appreciably greater than would be deduced from theory, although in each case the effect is of the sign that would be expected. For example, at —10° yaw, with the model turning with a negative angular velocity, the local angle of yaw* is less at the forward end of the model than at the centre. We should, therefore, expect the difference of pressure between the leeward and windward

* By the term "local angle of yaw at any point" is understood the angle between the axis of the model and the tangent to the circle in which that point is moving.

side of the equator to be less in curvilinear motion than in rectilinear motion. Fig. 16 shows that such is the case. Similarly at 10° yaw and a negative angular velocity, the local angle of yaw is greater at the forward end and a greater pressure difference between leeward and windward is noticed (fig. 17).

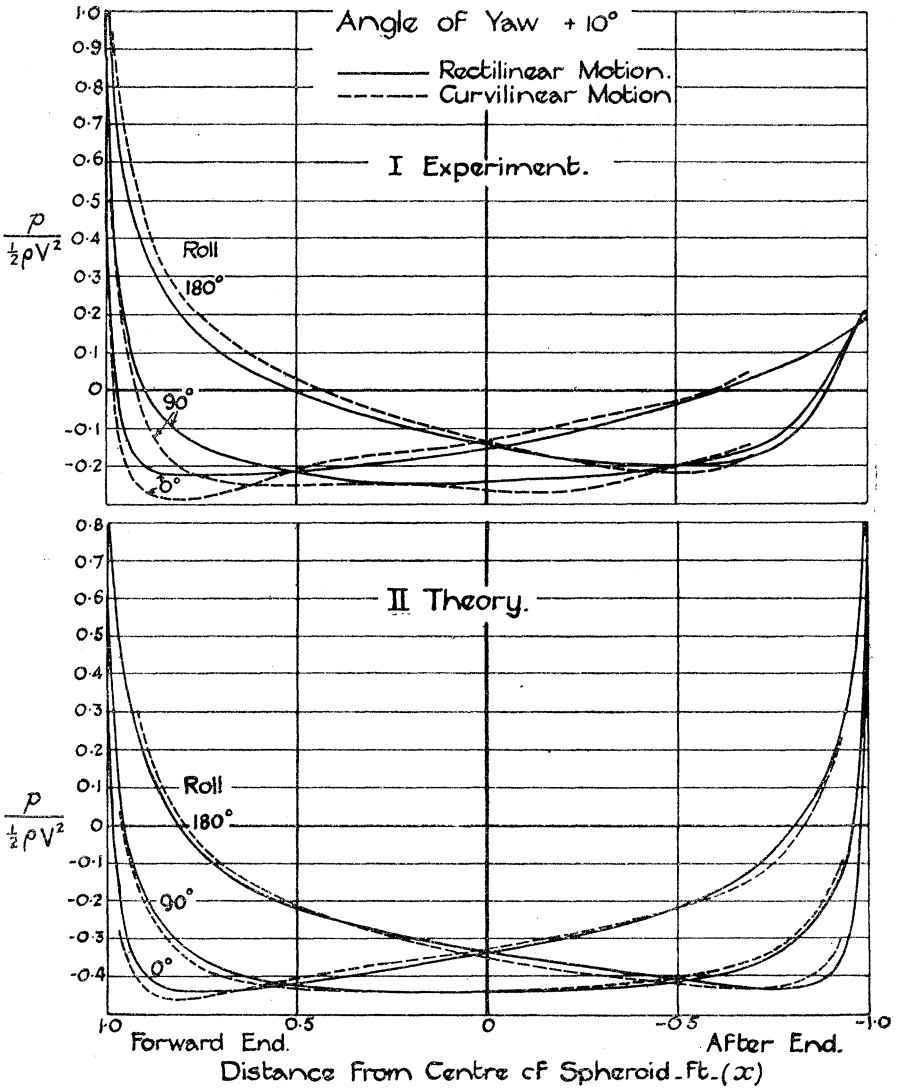

FIG. 17.—Comparison between Rectilinear and Curvilinear Motion. Angle of Yaw +10°.

27. It should be noted here that the contribution of the term in $1/R^2$ or Ω^2 in the expression (9) of Section I is practically negligible in the calculation of the theoretical pressures. Fig. 9 shows that the maximum value of the theoretical pressure on the spinning spheroid is $1{\cdot}86 \times \frac{\rho}{2} a^2\Omega^2$, or, if regarded as a contribution to the pressure on a spheroid moving in a circle, is $1{\cdot}86 \times \frac{\rho V^2}{2R^2}$, showing that the maximum magnitude of

the Ω^2 contribution to $p/\frac{1}{2}\rho V^2$ in the present case is 0·0024. Assuming that the experimental pressures can be expressed in the form

$$\tfrac{1}{2}\rho V^2 \,(k_1 + k_2/R + k_3/R^2)$$

(where k_3 is the experimental pressure coefficient in the case of the spinning spheroid), it appears that the term k_3/R^2 may be neglected.

28. Fig. 18 shows the average pressure at angles of yaw 0°, 10°, — 20° and + 20°.

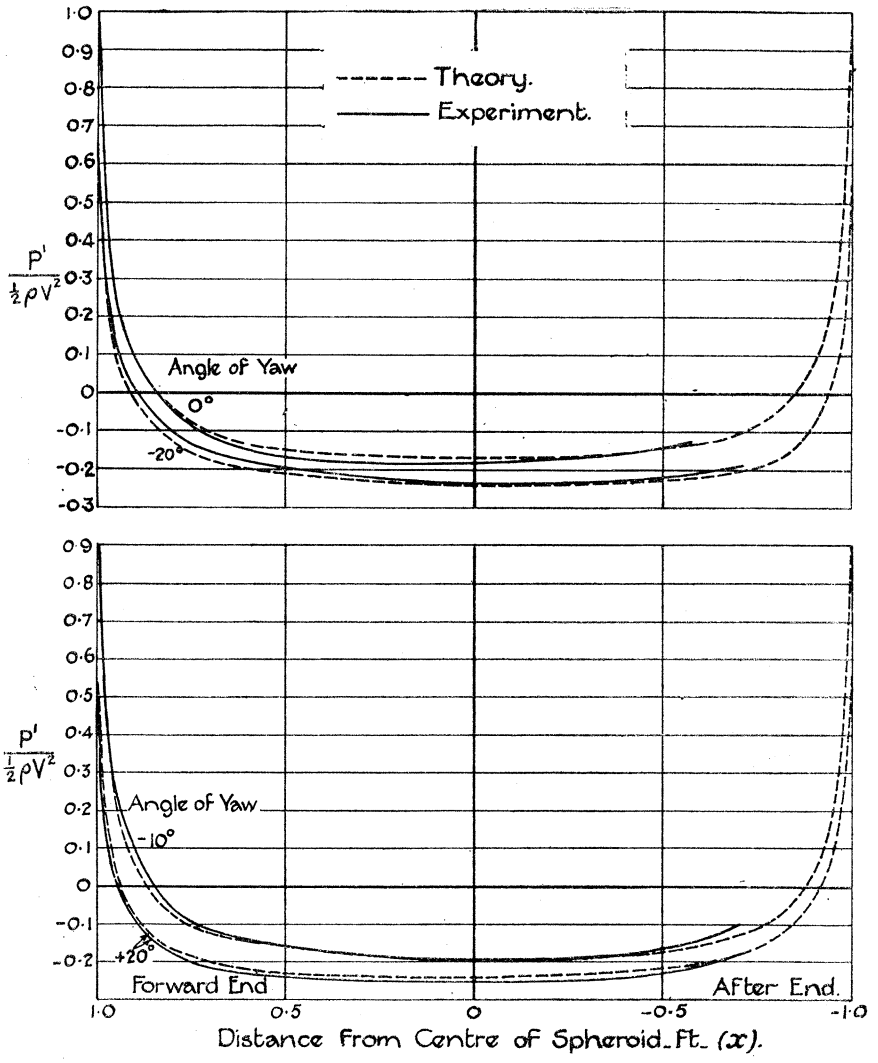

FIG. 18.—Average Pressures in Curvilinear Motion.

The agreement in this case compares very favourably with that obtaining in rectilinear motion (fig. 7).

Coming now to the resultant lateral pressures (fig. 19), we note one interesting difference

in the order of the agreement between theory and experiment in the two cases of rectilinear and curvilinear motion. A glance at fig. 8 shows that the magnitude of the discrepancy between theory and experiment at 20° yaw in the wind tunnel is roughly the same as that obtaining at 20° yaw on the whirling arm. But in the former case the discrepancy becomes less as the angle of yaw decreases, whereas in the latter it does not, the magnitude of the difference being approximately the same at the extreme forward end of the model for all angles of yaw. At zero yaw the resultant pressure vanishes in rectilinear motion; hence fig. 19 shows us the effect of rotation at zero yaw. For about

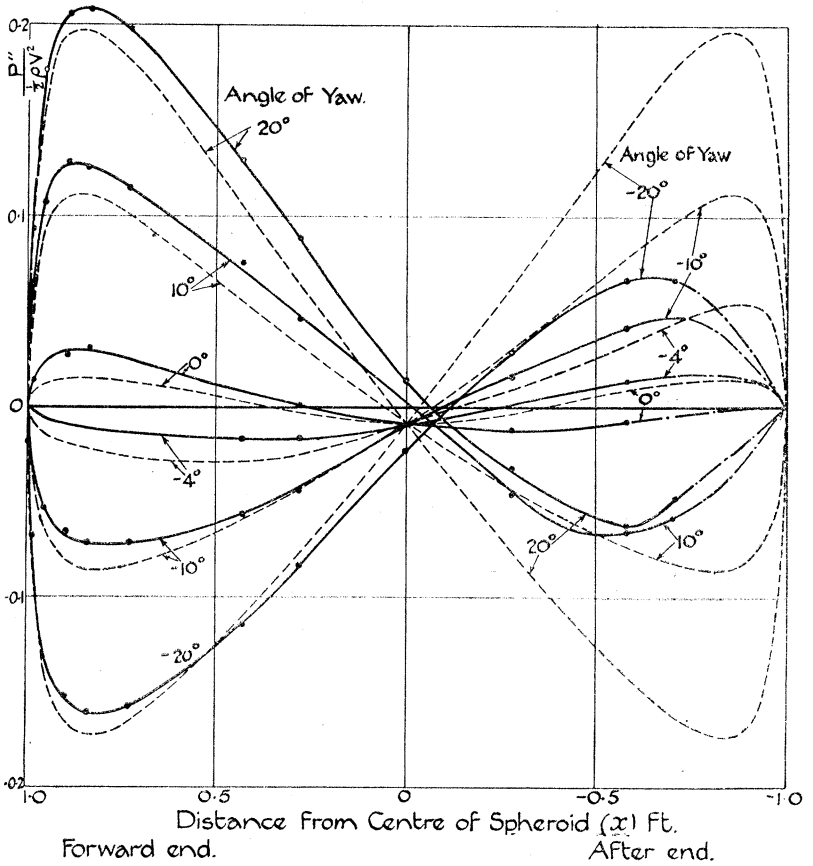

FIG. 19.—Resultant Lateral Pressures in Curvilinear Motion.

- - - - - Theory. ——— Experiment.

one-quarter of the length of the model the theoretical effect of rotation is about one-half of the actual. If we modify fig. 19 by altering the ordinates (when $0 < x < 1$) by the difference between the theoretical and experimental curves at zero yaw, we obtain fig. 20, in which the agreement between experiment and the modified theoretical curves is very good at the forward end of the model.

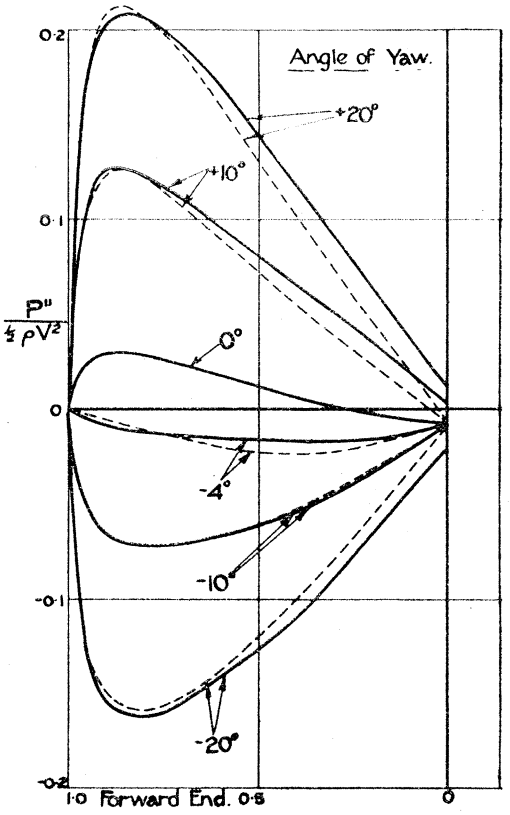

FIG. 20.—Resultant Lateral Pressures in Curvilinear Motion.
- - - - - Modified Theory. ——— Experiment.

29. In figs. 21 and 22 the curves of figs. 8 and 19 have been reproduced, but the experimental curves are now plotted on the one drawing and the theoretical curves on the other. The difference between the resultant pressures in rectilinear and curvilinear motion shows the same characteristic as that noted in connection with figs. 16 and 17—an increase in the magnitude of the pressure at the forward end at positive angles of yaw and a decrease at negative angles, corresponding with an increase and decrease in the local angle of yaw due to rotation. The effect of rotation, however, appears to be greater at negative angles (*i.e.*, at the angles corresponding with the attitude of an airship in curvilinear motion), but the sign changes between $x = 0{\cdot}2$ and $0{\cdot}3$. This indicates that a strip theory of the usual type could not be applied to estimate, from the pressures in rectilinear motion, the distribution of resultant pressures in curvilinear motion.

Another feature of these two figures is that whereas, according to theory, the effect of rotation is approximately the same at each angle of yaw (it varies as cos β—see equation 22, Section I), experiment shows a steady increase from 20° to — 20° yaw over the forward quarter of the model. It is roughly the same in both theory and experiment at 20° yaw, but about three times as great experimentally as it is theoretically at — 20° yaw when x is greater than $0{\cdot}7$.

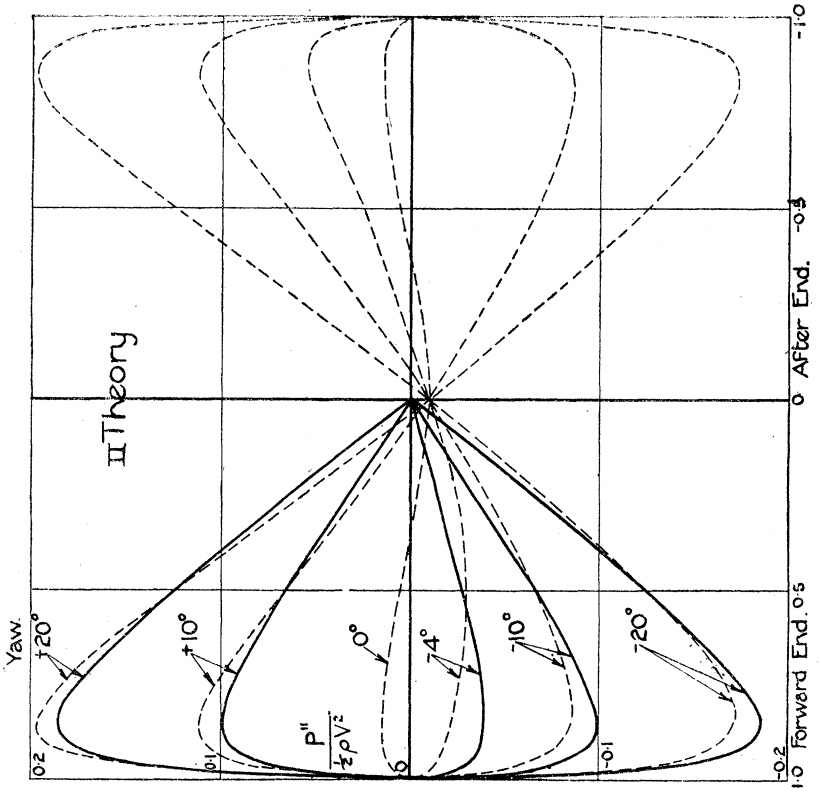

FIG. 22.

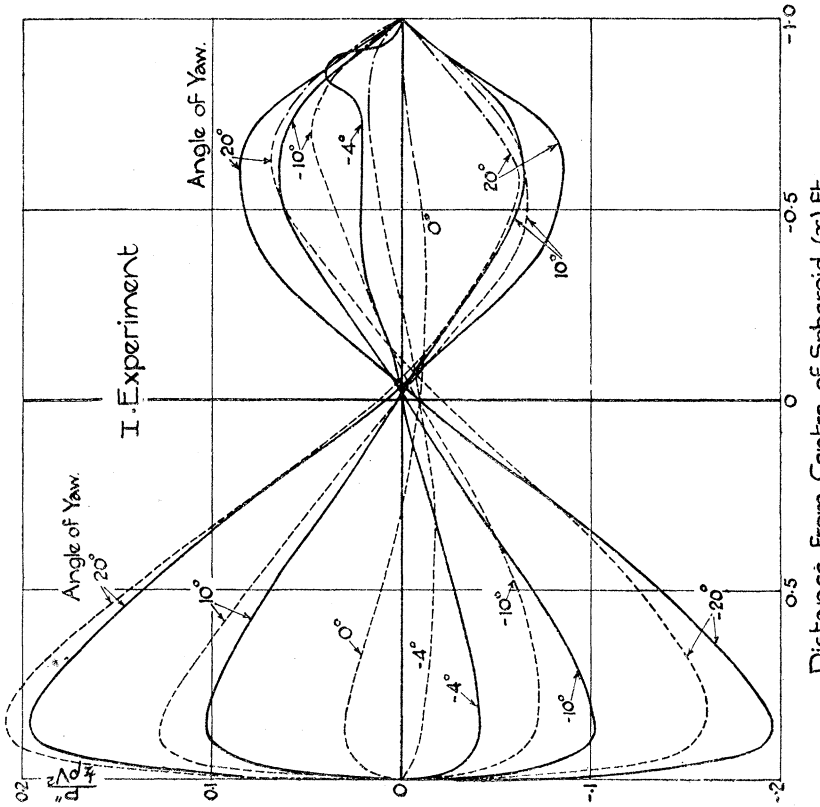

FIG. 21.

FIGS. 21 and 22.—Comparison of Resultant Lateral Pressure in Rectilinear and Curvilinear Motion, in Experiment and in Theory.

- - - - - Curvilinear Motion. ——— Rectilinear Motion.

Let us now consider the lateral force and yawing moment as deduced from the resultant pressures plotted in fig. 19. The values obtained are given in the following table, in which are also included the values previously given for rectilinear motion. The figures apply to the actual model, 2 feet long, moving at 40 feet per second.

Lateral Force in lbs.

Angle of yaw (degrees).	Deduced by integration.		Measured in wind tunnel.
	Curvilinear motion.	Rectilinear motion.	Rectilinear motion.
−20	−0·137	−0·127	−0·151
−10	$-0{\cdot}056_5$	$-0{\cdot}045_5$	$-0{\cdot}056_5$
− 4	−0·017	−0·012	$-0{\cdot}015_5$
0	0·003	0	0
10	0·066	$0{\cdot}045_5$	$0{\cdot}056_5$
20	0·183	0·127	0·151
Yawing Moment lbs.-ft.			
−20	−0·157	−0·207	−0·179
−10	−0·078	−0·122	−0·106
− 4	−0·018	−0·052	−0·045
0	0·021	0	0
10	0·127	0·122	0·106
20	0·177	0·207	0·179

These values are plotted in fig. 23.

It will be seen that the effect of rotation is to increase the magnitude of the lateral force throughout the range, except when $0 > \beta > -1°$ approximately. On the other hand, the yawing moment is less numerically when β has a negative value greater than 1°. At positive values of β below about 13°, rotation increases the yawing moment. Between $\beta = 0$ and $\beta = -1°$, the sign of the yawing moment differs in the two cases.

That the lateral force is numerically greater in curvilinear motion than in rectilinear motion throughout nearly the whole negative range may be an unexpected result. Fig. 21 shows the reason. Although the resultant pressure in the former case is numerically less over the greater part of the forward end, it is also less over the entire after-half, and thus the decrease in lateral force over the forward half is more than balanced by the effect of rotation on the after-half. In the case of yawing moment, instead of cancelling one another, the differences on both halves of the model are additive.

Finally, it is necessary to draw attention to the appreciable speed effect noticed in connection with the whirling-arm experiments. In general it is fairly consistent, and such as would tend to bring the experimental results at higher speeds into closer agreement with theory. The curves show the pressures obtained at the highest speed. The

number of observations, however, is so great that tables showing individual pressures are not included in the present paper. The figures have been selected to indicate the general nature of the results.

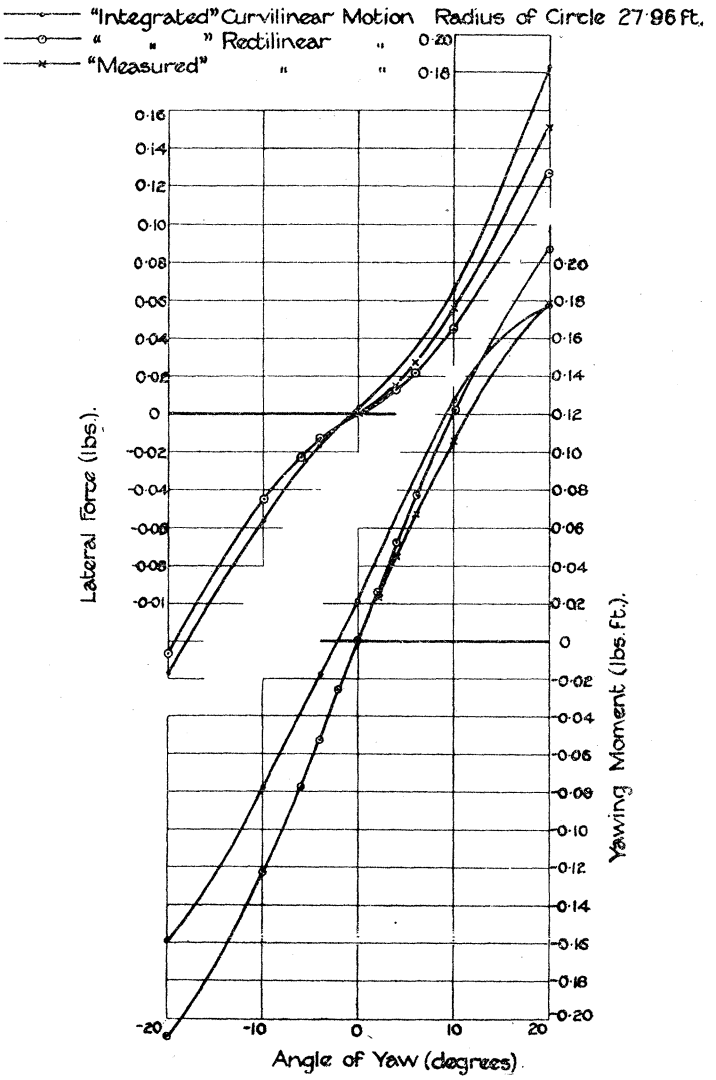

FIG. 23.—Lateral Force on the Model (2 feet long) at 40 ft./sec.

A complete set of tables will be found in the 'Aeronautical Research Committee's Reports and Memoranda No. 1061.'* Tables showing the resultant lateral pressures only are included in this paper.

In conclusion, the author desires to record his indebtedness to Mr. R. V. SOUTHWELL, F.R.S., for suggestions for overcoming the experimental difficulties encountered in connection with the whirling-arm experiments, and to Mr. A. H. BELL, who, jointly with the author, conducted the experimental work and reduced the results.

* In an appendix to this report will also be found details of the checks referred to in §§ 10 and 13.

TABLE I.—Resultant Lateral Pressures Normal to the Surface of a Prolate Spheroid. Rectilinear Motion. $*P_1''/\frac{1}{2}\rho V^2$ = the term independent of R in equation (23).

x ft.	Experiment. Angle of yaw (degrees). 2	4	6	10	20	x ft.	Theory. Angle of yaw (degrees). 2	4	6	10	20
1·0	0	0	0	0	0	1·0	0	0	0	0	0
0·999	—	—	—	—	—	0·999	0·0005	0·0011	0·0016	0·0026	0·0049
0·996	0·0022	0·0047	0·0064	0·0112	0·0215	0·997	0·0025	0·0050	0·0074	0·0122	0·0229
0·994	0·0047	0·0093	0·0139	0·0234	0·0445	0·993	0·0048	0·0096	0·0144	0·0236	0·0445
0·988	0·0086	0·0167	0·0253	0·0419	0·0792	0·988	0·0076	0·0151	0·0225	0·0371	0·0696
0·982	0·0100	0·0200	0·0310	0·0518	0·0964	0·982	0·0100	0·0199	0·0297	0·0488	0·0917
0·974	0·0125	0·0260	0·0386	0·0631	0·1155	0·974	0·0125	0·0250	0·0374	0·0613	0·1150
0·963	0·0157	0·0303	0·0457	0·0755	0·1425	0·965	0·0145	0·0289	0·0431	0·0710	0·1333
0·950	0·0168	0·0329	0·0482	0·0801	0·1530	0·952	0·0164	0·0327	0·0489	0·0804	0·1510
0·932	0·0181	0·0356	0·0536	0·0885	0·1676	0·932	0·0182	0·0363	0·0543	0·0893	0·1680
0·896	0·0199	0·0412	0·0614	0·1017	0·1911	0·894	0·0197	0·0393	0·0587	0·0967	0·1820
0·837	0·0210	0·0413	0·0616	0·1023	0·1950	0·838	0·0201	0·0401	0·0599	0·0985	0·1850
0·728	0·0195	0·0397	0·0578	0·0956	0·1820	0·729	0·0187	0·0374	0·0559	0·0919	0·1730
0·590	0·0156	0·0324	0·0482	0·0806	0·1560	0·586	0·0156	0·0312	0·0468	0·0766	0·1440
0·439	0·0127	0·0256	0·0388	0·0644	0·1280	0·431	0·0118	0·0236	0·0353	0·0579	0·1087
0·285	0·0087	0·0172	0·0242	0·0404	0·0837	0·279	0·0076	0·0153	0·0228	0·0375	0·0704
0·099	0·0025	0·0053	0·0095	0·0165	0·0345	0·087	0·0038	0·0048	0·0072	0·0118	0·0221
−0·099	—	—	−0·0027	−0·0035	−0·0117	−0·087	−0·0039	−0·0048	−0·0072	−0·0118	−0·0221
−0·285	−0·0098	−0·0169	−0·0252	−0·0354	−0·0549	−0·279	−0·0076	−0·0153	−0·0228	−0·0375	−0·0704
−0·439	−0·0118	−0·0224	−0·0324	−0·0537	−0·0743	−0·431	−0·0118	−0·0236	−0·0353	−0·0579	−0·1087
−0·590	−0·0097	−0·0207	−0·0354	−0·0652	−0·0849	−0·586	−0·0156	−0·0312	−0·0468	−0·0766	−0·1440
−0·728	−0·0085	−0·0212	−0·0385	−0·0590	−0·0745	−0·729	−0·0187	−0·0374	−0·0559	−0·0919	−0·1730
−0·837	−0·0226	−0·0382	−0·0424	−0·0442	−0·0696	−0·838	−0·0201	−0·0401	−0·0599	−0·0985	−0·1850
−0·950	—	−0·0011	−0·0016	−0·0042	−0·0130	−0·952	−0·0164	−0·0327	−0·0489	−0·0804	−0·1510
−0·994	—	+0·0009	+0·0010	+0·0005	−0·0027	−0·993	−0·0048	−0·0096	−0·0144	−0·0236	−0·0445
−0·996	−0·0003	0·0004	0·0007	0·0003	−0·0019	−0·997	−0·0025	−0·0050	−0·0074	−0·0122	−0·0229
−0·999	0·0001	0·0003	0·0004	0·0002	−0·0010	−0·999	−0·0005	−0·0011	−0·0016	−0·0026	−0·0049
−1·0	0	0	0	0	0	−1·0	0	0	0	0	0

* P in these tables is in lbs./ft., V in ft./sec., Ω in rads./sec., a in feet and $\rho = 0{\cdot}00237$ slugs/cu. ft.

TABLE II.—Resultant Lateral Pressures Normal to the Surface of a Prolate Spheroid. Spinning Motion. Experiment. $P_3''/\frac{1}{2}\rho a^2\,\Omega^2$.

x ft.	Angular velocity Ω (rads./sec).			
	7·6	14·7	27·8	39·5
1·0	0	0	0	0
0·937	0·047	0·055	0·055	0·052
0·832	0·174	0·182	0·175	0·163
0·748	0·191	0·178	0·156	0·141
0·580	0·125	0·107	0·088	0·081
0·409	0·066	0·064	0·053	0·047
0·229	—	0·025	0·025	0·021
0	0	0	0	0

Theoretically the resultant lateral pressures are zero throughout as there is no term in $1/R^2$ in equation (23), § 13.

TABLE III.—Resultant Lateral Pressures Normal to the Surface of a Prolate Spheroid. Curvilinear Motion. Experiment. $P''/\frac{1}{2}\rho V^2$.

Radius of Turning Circle R = − 27·96′. Length of Spheroid 2′.

x ft.	Angle of yaw (degrees).					
	−20	−10	−4	0	+10	+20
1·0	0	0	0	0	0	0
0·997	0·0199	0·0090	0·0014	−0·0042	0·0086	—
0·985	0·0684	0·0291	0·0025	−0·0148	0·0590	0·093
0·951	0·1287	0·0530	0·0065	−0·0260	0·1105	0·176
0·894	0·1512	0·0653	0·0073	−0·0276	0·1290	0·205
0·836	0·1610	0·0715	0·0087	−0·0312	0·1260	0·207
0·727	0·1570	0·0707	0·0135	−0·0236	0·1215	0·198
0·429	0·1175	0·0570	0·0172	—	0·0760	0·129
0·278	0·0833	0·0450	0·0167	0	0·0460	0·089
0	0·0247	0·0070	0·0110	+0·0085	0·0050	0·014
−0·278	−0·0275	−0·0155	—	0·0132	−0·0460	0·033
−0·583	−0·0640	−0·0411	−0·0137	0·0075	−0·0650	$-0{\cdot}054_5$
−0·705	−0·0645	−0·0470	−0·0116	0	−0·0580	$-0{\cdot}050_7$

TABLE IV.—Resultant Lateral Pressures ($P''/\frac{1}{2}\rho V^2$) Normal to the Surface of a Prolate Spheroid.

Curvilinear Motion. Theory.

Radius of Turning Circle R = — 27·96′. Length of Spheroid = 2′.

x ft.	β angle of yaw (degrees).								
	—20	—10	—6	—4	0	4	6	10	20
1·0	0	0	0	0	0	0	0	0	0
0·997	—0·0209	—0·0100	—0·0052	—0·0027	0·0022	0·0072	0·0056	0·0144	0·0251
0·982	—0·0836	—0·0403	—0·0213	—0·0112	0·0086	0·0285	0·0353	0·0573	0·0998
0·964	—0·1220	—0·0590	—0·0311	—0·0167	0·0122	0·0411	0·0553	0·0830	0·1450
0·932	—0·1540	—0·0749	—0·0399	—0·0219	0·0144	0·0505	0·0685	0·1033	0·1810
0·838	—0·1746	—0·0860	—0·0474	—0·0275	0·0127	0·0529	0·0726	0·1110	0·1984
0·729	—0·1653	—0·0838	—0·0478	—0·0292	0·0082	0·0456	0·0640	0·1000	0·1807
0·586	—0·1418	—0·0744	—0·0444	—0·0289	0·0023	0·0335	0·0490	0·0790	0·1462
0·431	—0·1108	—0·0602	—0·0378	—0·0263	—0·0030	0·0203	0·0318	0·0544	0·1052
0·279	—0·0766	—0·0439	—0·0293	—0·0218	—0·0066	0·0086	0·0163	0·0309	0·0642
0	—0·0087	—0·0092	—0·0092	—0·0093	—0·0093	—0·0093	—0·0092	—0·0092	—0·0087

When x is negative, interchange the signs of β.

TABLE V.—Resultant Lateral Pressures Normal to the Surface of a Prolate Spheroid.

Effect of Rotation. Theory.

Table giving the values of $\frac{R}{a} \cdot \frac{P_2''}{\frac{1}{2}\rho V^2} = \frac{P_2''}{\frac{1}{2}\rho a \Omega V}$,

where R = the radius of turning circle, Ω the angular velocity, and a the semi-major axis of the spheroid.

x ft.	Angle of yaw β (degrees).					
	0	2	4	6	10	20
1·0	0	0	0	0	0	0
0·997	—0·062	—0·062	—0·062$_5$	—0·062	—0·061$_5$	—0·059
0·982	—0·242	—0·242	—0·241	—0·240	—0·238	—0·228
0·964	—0·342	—0·342	—0·341	—0·339	—0·337	—0·321
0·932	—0·402	—0·402	—0·401	—0·400	—0·396	—0·378
0·838	—0·356	—0·356	—0·355	—0·352	—0·350	—0·334
0·729	—0·230	—0·230	—0·230	—0·228	—0·226	—0·216
0·586	—0·064$_5$	—0·064$_5$	—0·064$_5$	—0·064	—0·063$_5$	—0·060$_5$
0·431	+0·083	+0·083	+0·083	+0·082	+0·081$_5$	+0·078
0·279	0·185	0·185	0·185	0·185	0·182	0·174
0	0·261	0·261	0·260	0·259	0·257	0·245

P_2'' is the term in 1/R in equation (23) of § 13.

The sign changes with the sign of β, but not with the sign of x.